Transactions Papers

OFDM or Single-Carrier Block Transmissions?

Zhengdao Wang, *Member, IEEE*, Xiaoli Ma, *Member, IEEE*, and Georgios B. Giannakis, *Fellow, IEEE*

***Abstract*—We compare two block transmission systems over frequency-selective fading channels: orthogonal frequency-division multiplexing (OFDM) versus single-carrier modulated blocks with zero padding (ZP). We first compare their peak-to-average power ratio (PAR) and the corresponding power amplifier backoff for phase-shift keying or quadrature amplitude modulation. Then, we study the effects of carrier frequency offset on their performance and throughput. We further compare the performance and complexity of uncoded and coded transmissions over random dispersive channels, including Rayleigh fading channels, as well as practical HIPERLAN/2 indoor and outdoor channels. We establish that unlike OFDM, uncoded block transmissions with ZP enjoy maximum diversity and coding gains within the class of linearly precoded block transmissions. Analysis and computer simulations confirm the considerable edge of ZP-only in terms of PAR, robustness to carrier frequency offset, and uncoded performance, at the price of slightly increased complexity. In the coded case, ZP is preferable when the code rate is high (e.g., $3/4$), while coded OFDM is to be preferred in terms of both performance and complexity when the code rate is low (e.g., $1/2$) and the error-correcting capability is enhanced. As ZP block transmissions can approximate serial single-carrier systems as well, the scope of the present comparison is broader.**

***Index Terms*—Capacity, coding, diversity, frequency-selective fading, HIPERLAN, multicarrier, orthogonal frequency-division multiplexing (OFDM), peak-to-average ratio (PAR), single carrier, synchronization.**

I. Introduction

ORTHOGONAL frequency-division multiplexing (OFDM) has already been included in digital audio/video broadcasting (DAB/DVB) standards in Europe, and has been successfully applied to high-speed digital subscriber line (DSL) modems in the United States. Recently, it has also been proposed for digital cable television systems and local area mobile wireless networks, such as those specified in the IEEE802.11a, and the HIPERLAN/2 standards [16]. By implementing an inverse fast Fourier transform (IFFT) at the transmitter and a fast Fourier transform (FFT) at the receiver, OFDM converts an intersymbol interference (ISI) channel into parallel ISI-free subchannels with gains equal to the channel's frequency response values on the FFT grid. To eliminate interblock interference (IBI) between successive IFFT-processed blocks, a cyclic prefix (CP) of length no less than the channel order is inserted per transmitted block. Discarding the CP at the receiver not only suppresses IBI, but also converts the linear channel convolution into circular convolution, which facilitates diagonalization of the associated channel matrix (see, e.g., [44]).

Although OFDM enables simple equalization, it introduces the following three well-known problems.

1) The peak-to-average ratio (PAR) of the transmitted signal power is large, necessitating power backoff, unless PAR-reduction techniques are incorporated to control the resulting nonlinear distortion at the power-amplification stage.
2) Because information symbols are transmitted on subcarriers, OFDM is sensitive to transmit–receive oscillators' mismatch and Doppler effects, both of which cause (sub)carrier frequency offset (CFO).
3) Uncoded OFDM does not enable the available multipath (or frequency) diversity. In fact, only diversity order one is possible through multipath Rayleigh fading channels; see, e.g., [5] and [45].

To alleviate problem 1), several PAR-reduction algorithms have been devised [6], [27], [35], [43]. But the resulting PARs are still at least a few decibels larger than those of serial single-carrier transmissions. Therefore, time-domain amplitude clipping is often performed to mitigate the PAR effects problem [4], [6], [12], [13], [21], [26], [27], [33]–[35], [43], [51] . The problem with 2), i.e., OFDM's sensitivity to subcarrier offsets, poses challenges in OFDM applications to time-varying scenarios, and requires tight carrier synchronization. To mitigate the loss of diversity, the problem in 3), dependence among symbols on different subcarriers, can be introduced either through linear precoding over the complex field (as in, e.g., [45]), or more commonly, by invoking Galois field (block or convolutional) channel coding, as in [17]. When Galois field error-control codes are applied, existing soft-decision decoding algorithms, such as the Viterbi algorithm (VA), are used for decoding coded OFDM symbols with only minor modifications in computing the VA metrics. However, relying on error-control

Paper approved by C. Tellambura, the Editor for Modulation and Signal Design of the IEEE Communications Society. Manuscript received August 16, 2001; revised April 3, 2003. This work was supported in part by the National Science Foundation (NSF) under Grant 01-0516, and in part by the Applied Research Laboratory/Collaborative Technology Alliance (ARL/CTA) under Grant DAAD19-01-2-011. This paper was presented in part at the IEEE Wireless Communications and Networking Conference, Orlando, FL, March 17–21, 2002.

Z. Wang is with the Department of Electrical and Computer Engineering, Iowa State University, Ames, IA 50011 USA (e-mail: zhengdao@iastate.edu).

X. Ma is with the Department of Electrical and Computer Engineering, Auburn University, Auburn, AL 36849 USA (e-mail: xiaoli@eng.auburn.edu).

G. B. Giannakis is with the Department of Electrical and Computer Engineering, University of Minnesota, Minneapolis, MN 55455 USA (e-mail: georgios@ece.umn.edu).

Digital Object Identifier 10.1109/TCOMM.2004.823586

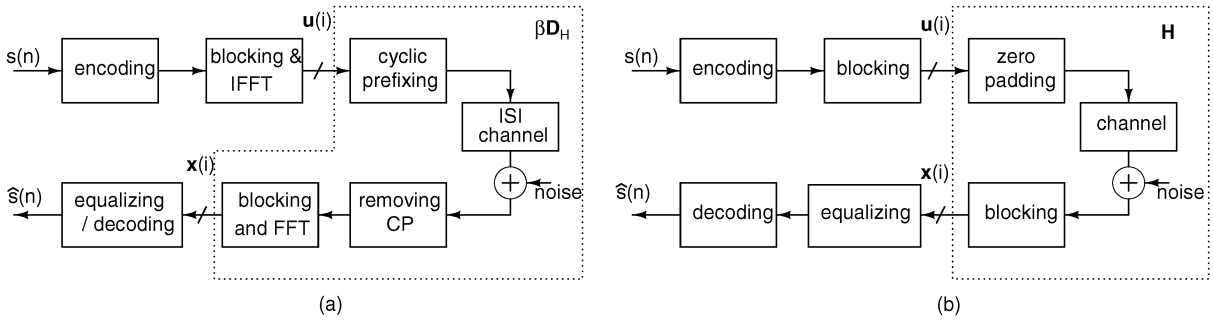

Fig. 1. (a) OFDM transceiver. (b) Single-carrier block transceiver.

codes to pick up the performance loss in diversity curtails the codes' ability to cope with other impairments caused by, e.g., additive noise and nonlinear distortions. It has been shown recently that carefully designed linear precoding is also effective in dealing with frequency selectivity [45]. An interesting linear precoder actually annihilates the IFFT at the transmitter, and lends itself to a single-carrier zero-padded (ZP) block transmission system [40], [45]. This system will henceforth be referred to as the ZP-only system, or ZP-only for brevity. A ZP-only transmission is essentially a serial single-carrier transmission, except that a number of zeros (guard symbols) are inserted periodically in the symbol stream.

In this paper, we will place OFDM and ZP-only under a common denominator, and compare them in various practical and theoretical aspects, including 1)–3) above. There have been works on comparing multicarrier with single-carrier systems. In [8], [11], [48], and [53], performance of optimized multicarrier transmissions with channel state information (CSI) at the transmitter is studied and compared against single-carrier transmissions with linear or decision-feedback equalization (DFE) for fixed dispersive channels. With CSI available at the transmitter, multicarrier alternatives outperform single-carrier transmissions, while having comparable, or even lower, complexity. In [3], the cutoff rate is used to compare linearly equalized single-carrier transmissions against coded OFDM over random channels. Tradeoffs between performance and complexity of trellis-coded multicarrier versus single-carrier systems with minimum mean-squared error (MMSE) DFE are studied thoroughly in [23], where it is shown that a single-carrier system is slightly favorable when the code rate is high, while a multicarrier system is slightly favorable when the code rate is low.

Our work in this paper can be viewed as building on the work of [39], where the effects of nonlinear distortion, carrier-frequency offset, and error-control coding on single- and multicarrier systems are also compared. Our comparison differs from the previous studies in [23] and [39] in the following aspects:

a) while existing works focus on serial single-carrier transmissions, we focus on *block zero-padded* single-carrier transmissions, and substantiate analytically their merits with respect to maximum diversity and coding gains;
b) we conduct quantitative PAR comparisons for OFDM and ZP-only for various constellations;
c) we quantify the effects of CFO on bit-error rate (BER) performance and information throughput;
d) we rely on standard HIPERLAN/2 channel models for simulation (unlike [39], which uses fixed channels).

We will use block MMSE-DFE and simple linear equalization for our single-carrier ZP-only transmissions. Despite the *block* nature of ZP-only, it can approximately represent serial single-carrier (SSC) transmissions without ZP. Although the latter does not guarantee existence of a linear zero-forcing (ZF) equalizer, simulations reveal that its performance with a serial MMSE-DFE equalizer is quite close to the block ZP-only system with block MMSE-DFE, when ZP occupies only a small fraction of the transmission block, and the feed-forward filter for the serial MMSE-DFE is long enough. The PAR and sensitivity to CFO for the SSC transmissions without ZP are essentially the same as those of a block ZP-only system, provided that the ZP guard is relatively small. These considerations qualify ZP-only as a single-carrier benchmark system for comparison with OFDM. The block nature of ZP-only, however, does allow one to simplify and unify SSC and OFDM system models, and derive corresponding equalizers and figures of merit (BER and mutual information rate), in addition to guaranteeing the existence of linear ZF equalization.

II. System Modeling

Notation: Bold uppercase letters denote matrices and lowercase letters denote column vectors; $\star, (\cdot)^{\dagger}, (\cdot)^{T}$, and $(\cdot)^{\mathcal{H}}$ denote convolution, pseudoinverse, transpose, and Hermitian transpose, respectively; $[\cdot]_{i,j}$ denotes the (i,j)th entry of a matrix; $\mathbf{I}_M$ denotes identity matrix of size M; $\mathrm{diag}(\mathbf{x})$ is a diagonal matrix with $\mathbf{x}$ on its diagonal; $\mathrm{E}[\cdot]$ denotes expectation. We always index matrix and vector entries starting from 0. For a vector, $\|\cdot\|$ denotes the Euclidean norm, and $\|\cdot\|_{\infty}$ its infinite norm (the maximum amplitude of its entries). For a set, $|\cdot|$ denotes its cardinality. The complex set is denoted as $\mathbb{C}$; and the real and imaginary parts are denoted as $\Re\{\cdot\}$ and $\Im\{\cdot\}$, respectively.

A. OFDM System Model

In OFDM transmissions [see Fig. 1(a)], a serial stream $s(n)$ of information symbols is first passed through an error-control encoder, whose output is denoted[1] as $u(n)$. In the uncoded case, $u(n) = s(n)$. The sequence $u(n)$ is then grouped in blocks of

[1]For simplicity, we use index n for symbol streams of possibly different rates.

size $N, \mathbf{u}(i) := [u(iN), u(iN+1), \ldots, u(iN+N-1)]^T$, to which an IFFT is performed to obtain

$$\tilde{\mathbf{u}}(i) := \mathbf{F}^{\mathcal{H}}\mathbf{u}(i) \tag{1}$$

where $\mathbf{F}$ is the $N \times N$ FFT matrix with $[\mathbf{F}]_{n,k} = N^{-(1/2)} \exp(-j2\pi nk/N)$. A CP of length $L_{\rm cp}$ is then inserted in $\tilde{\mathbf{u}}(i)$ to yield $\tilde{\mathbf{u}}_{\rm cp}(i) := \beta \mathbf{T}_{\rm cp}\tilde{\mathbf{u}}(i)$ of length $P := N + L_{\rm cp}$, where $\mathbf{T}_{\rm cp} := [\mathbf{I}_{\rm cp}^T \mathbf{I}_N^T]^T$ describes the CP insertion by concatenating the last $L_{\rm cp}$ rows of an $N \times N$ identity matrix $\mathbf{I}_N$ (that we denote as $\mathbf{I}_{\rm cp}$) with the identity matrix $\mathbf{I}_N$ itself; the *power loss factor*

$$\beta := \sqrt{N/P} \tag{2}$$

is used to maintain the same power before and after CP insertion. The block $\tilde{\mathbf{u}}_{\rm cp}(i)$ of length P is serialized to yield $\tilde{u}_{\rm cp}(n)$, which is pulse shaped, carrier modulated, power amplified, and transmitted through the channel. Our baseband discrete-time-equivalent model combines the effects of the spectral-shaping pulse, the continuous-time channel, the receive-filter, and symbol-rate sampling as a discrete-time causal finite-impulse response (FIR) channel with impulse response $h(n)$, and order L that is upper bounded by $L_{\rm cp}$ (see, e.g., [37] for details). Perfect symbol and block synchronization is assumed.

With a square-root Nyquist receive filter, the symbol rate samples can be written as $x(n) = \tilde{u}_{\rm cp}(n) \star h(n) + v(n)$, where $v(n)$ is additive white Gaussian noise (AWGN). The samples $x(n)$ are grouped into blocks of size P as $\mathbf{x}_{\rm cp}(i) := [x(iP), x(iP+1), \ldots, x(iP+P-1)]^T$. The first $L_{\rm cp}$ entries of $\mathbf{x}_{\rm cp}(i)$ corresponding to the CP are removed, leaving us with blocks $\mathbf{x}(i) := [x(iP+L_{\rm cp}), x(iP+L_{\rm cp}+1), \ldots, x(iP+P-1)]^T$ of length N. We define $\tilde{\mathbf{H}}$ to be an $\mathrm{N} \times \mathrm{N}$ circulant matrix with $[\tilde{\mathbf{H}}]_{n,k} = h((n-k)_{\rm mod N})$. The resulting block input–output relationship is $\tilde{\mathbf{x}}(i) = \beta\tilde{\mathbf{H}}\tilde{\mathbf{u}}(i) + \tilde{\boldsymbol{\eta}}(i)$, where $\tilde{\boldsymbol{\eta}}(i) := [v(iP+L_{\rm cp}), v(iP+L_{\rm cp}+1), \ldots, v(iP+P-1)]^T$ is the AWGN block. Applying FFT to $\tilde{\mathbf{x}}(i)$ brings us to $\mathbf{x}(i) := \mathbf{F}\tilde{\mathbf{x}}(i) = \beta\mathbf{F}\tilde{\mathbf{H}}\mathbf{F}^{\mathcal{H}}\mathbf{u}(i) + \tilde{\boldsymbol{\eta}}(i)$ [cf. (1)], or

$$\mathbf{x}(i) = \beta\mathbf{D}_H\mathbf{u}(i) + \boldsymbol{\eta}(i) \tag{3}$$

where

$$\mathbf{D}_H := \mathrm{diag}[H(e^{j0}), H(e^{j(2\pi/N)}), \ldots H(e^{j(2\pi(N-1)/N)})] = \mathbf{F}\tilde{\mathbf{H}}\mathbf{F}^{\mathcal{H}}$$

and $H(e^{j2\pi f})$ is the frequency response of the ISI channel; i.e., $H(e^{j2\pi f}) := \sum_{n=0}^{L_{\rm cp}} h(n)\exp(-j2\pi fn)$. An equalizer followed by a decoder will rely on $\mathbf{x}(i)$ to obtain estimates of the information symbols that were encoded into $\mathbf{u}(i)$.

In practical OFDM systems, not all subcarriers are used for transmission of information symbols; that is, other than carrying information symbols, some subcarriers can be used as a frequency guard band [1], [16], pilot tones for channel estimation [1], [16], and reserved tones for PAR reduction, e.g., [30].

B. ZP-Only System Model

Our ZP-only transmissions [see Fig. 1(b)] are different from OFDM in two aspects: 1) IFFT is not used; and 2) the CP is replaced by ZP. Specifically, to each encoded symbol block $\mathbf{u}(i), L_{\rm zp}$, zero symbols are appended before transmission. The system is called ZP-only because only ZP occurs at the transmitter—no Fourier transform is involved. We set $L_{\rm zp} = L_{\rm cp}$ so that the symbol rate of ZP-only and OFDM is kept the same. The $L_{\rm zp}$ zeros serve to separate two successive blocks so that no IBI emerges. Such ZP transmissions are the *digital* counterparts of what are more commonly known as transmissions with guard time (see, e.g., [37, p. 720]). The benefit of ZP *serial analog* transmissions has been appreciated for, e.g., suppressing adjacent channel interference; but it was not until recently that the importance of ZP *digital block* transmissions was revealed in [22], [40], [41], [44], and [45].

At the ZP-only receiver, we observe the entire linear convolution of length $N + L_{\rm zp} = P$ of each transmitted block with the channel. Denoting the ith observed block as $\mathbf{y}(i)$, we can relate it to $\mathbf{u}(i)$ via

$$\mathbf{y}(i) = \mathbf{H}\mathbf{u}(i) + \boldsymbol{\xi}(i) \tag{4}$$

where $\mathbf{H}$ is now a $P \times N$ Toeplitz convolution matrix with $[\mathbf{H}]_{p,n} = h(p-n)$, and $\boldsymbol{\xi}(i) := [v(iP), v(iP+1), \ldots, v(iP+P-1)]^T$ is the AWGN. Equalization and decoding are subsequently performed on $\mathbf{y}(i)$.

C. Similarities and Differences

OFDM's input–output relationship (3) and that of ZP-only in (4) will be our basis for comparison. From a unifying input–output perspective, both schemes can be viewed as passing an encoded input symbol block $\mathbf{u}(i)$ through a multiple-input/multiple-output (MIMO) channel that is corrupted by AWGN. The differences are as follows.

1) For OFDM, the output $\mathbf{x}(i)$ is of length N, while for ZP-only, $\mathbf{y}(i)$ has size $P = N + L_{\rm cp}$. Correspondingly, the AWGN blocks, $\boldsymbol{\eta}(i)$ and $\boldsymbol{\xi}(i)$, have different lengths, but their entries have the same variance $\sigma_v^2 = N_0$, where $N_0/2$ is the noise power spectrum density, because the FFT is a norm-preserving linear transform.
2) The mixing channel matrices are different. OFDM has a diagonal, possibly singular matrix $\mathbf{D}_H$ as its MIMO channel ($\mathbf{D}_H$ loses rank when there is a channel null on one of the FFT frequencies), while ZP-only comes with a Toeplitz matrix that has full rank (see, e.g., [40]) for all but the trivial null channel with all-zero taps. This full-rank property will give ZP-only an edge in performance relative to OFDM.

In addition to ZP-only, other single-carrier systems that share many of its properties (e.g., low PAR and insensitivity to CFO), include the SSC transmissions without ZP, and SSC transmission with CP [9], [39], which also afford low-complexity frequency-domain equalization. For simplicity and uniformity, we will be focusing on ZP-only in the comparisons. But our conclusions, except for those pertaining to diversity and coding gains in Section V-B, also apply to these other single-carrier schemes. We will verify the probability of error performance of various single-carrier schemes with different equalizers in Section V-B.

Based on their system models, we will compare OFDM with ZP-only in the following aspects: 1) PAR (Section III); 2) sensitivity to CFO or Doppler (Section IV); 3) uncoded system performance and complexity (Section V); and 4) coded system performance and complexity (Section VI).

III. Peak-to-Average Power Ratio (PAR)

OFDM transmissions exhibit large amplitude variations, which cause intercarrier modulation and out-of-band radiation. To study these effects, we need to take into account the spectral shaping pulse, and examine the continuous-time transmitted signal. To facilitate our discrete-time analysis, we will first consider a case where a Nyquist spectral shaping pulse is used, and the continuous-time signal is sampled at symbol rate. The effects of spectral shaping pulse and the continuous-time PAR will be examined using simulations.

A. Nyquist Pulse and Symbol-Rate Sampling

To simplify the problem, in this section, consider a Nyquist pulse and study the PAR for the symbol-rate sampled discrete-time signal. As confirmed by simulations, the PAR values derived here will be smaller than those of the actual continuous-time waveform by 1–2 dB. We will present these simulations in the next section.

We assume that the symbols in $\mathbf{u}(i)$ belong to a finite alphabet $\mathcal{A}$. Let us define the maximum amplitude $A_{\max} := \max_{\alpha\in\mathcal{A}} |\alpha|$, and the average energy per symbol as $\sigma_u^2 = (1/|\mathcal{A}|)\sum_{\alpha\in\mathcal{A}} |\alpha|^2$. The *instantaneous PAR* for the ith OFDM block, and the *overall PAR* (or simply PAR) are defined, respectively, by

$$\mathrm{PAR}_i^{\mathrm{ofdm}} := \frac{\|\tilde{\mathbf{u}}_{\mathrm{cp}}(i)\|_\infty^2}{\mathrm{E}\|\tilde{\mathbf{u}}_{\mathrm{cp}}(i)\|^2/P} \tag{5}$$

$$\mathrm{PAR}^{\mathrm{ofdm}} := \frac{\max_i \|\tilde{\mathbf{u}}_{\mathrm{cp}}(i)\|_\infty^2}{\mathrm{E}\|\tilde{\mathbf{u}}_{\mathrm{cp}}(i)\|^2/P}. \tag{6}$$

Notice that $\mathrm{PAR}^{\mathrm{ofdm}}$ is a deterministic quantity, while $\mathrm{PAR}_i^{\mathrm{ofdm}}$ is a random variable depending on each specific realization of the symbol block $\tilde{\mathbf{u}}_{\mathrm{cp}}(i)$.

In accordance with (5), the corresponding PAR expressions for the ith transmitted ZP-only block are, respectively

$$\mathrm{PAR}_i^{\mathrm{zp}} := \frac{\|\mathbf{u}(i)\|_\infty^2}{\mathrm{E}\|\mathbf{u}(i)\|^2/P} \quad \text{and} \quad \mathrm{PAR}^{\mathrm{zp}} := \frac{\max_i \|\mathbf{u}(i)\|_\infty^2}{\mathrm{E}\|\mathbf{u}(i)\|^2/P}. \tag{7}$$

In practice, the symbols in $\mathcal{A}$ typically occur with the same frequency in the coded symbol block $\mathbf{u}(i)$. We assume this is true to simplify our analysis. First, we compare $\mathrm{PAR}^{\mathrm{ofdm}}$ with $\mathrm{PAR}^{\mathrm{zp}}$. For OFDM, $\max_i \|\tilde{\mathbf{u}}(i)_{\mathrm{cp}}\|_\infty^2 = \max_i \|\mathbf{F}^{\mathcal{H}}\mathbf{u}(i)\|_\infty^2 = \max_{i,k} |(1/\sqrt{N})\sum_{n=0}^{N-1} u(iN+n)e^{j2\pi nk/N}|^2 = NA_{\max}^2$, where the maximum is achieved when $u(iN+n) = u(iN), n = 0, 2, \ldots, N-1$, and $|u(iN)| = A_{\max}$. Also, $\mathrm{E}[\|\tilde{\mathbf{u}}_{\mathrm{cp}}(i)\|] = (P/N)\mathrm{E}[\|\tilde{\mathbf{u}}(i)\|] = (P/N)\mathrm{E}[\|\mathbf{F}^{\mathcal{H}}\mathbf{u}(i)\|] = (P/N)\mathrm{E}[\|\mathbf{u}(i)\|] = P\sigma_u^2$. Thus, by definition, we find

$$\mathrm{PAR}^{\mathrm{ofdm}} = \frac{NA_{\max}^2}{\sigma_u^2}. \tag{8}$$

While for ZP-only, we have

$$\mathrm{PAR}^{\mathrm{zp}} = \frac{A_{\max}^2}{(N\sigma_u^2/P)} = \frac{PA_{\max}^2}{N\sigma_u^2}. \tag{9}$$

Comparing OFDM with ZP-only, it is easy to see that

$$\mathrm{PAR}^{\mathrm{ofdm}} = \frac{N^2}{P}\mathrm{PAR}^{\mathrm{zp}}.$$

It can be readily shown that:

TABLE I
PAR Comparison of OFDM Versus ZP-Only

constellation	$A_{\max}$	σ_u^2	$\mathrm{PAR}^{\mathrm{ofdm}}$	$\mathrm{PAR}^{\mathrm{zp}}$	$\mathrm{PAR}^{\mathrm{ofdm}}/\mathrm{PAR}^{\mathrm{zp}}$
PSK	1	1	18.06 dB	0.97 dB	17.09 dB
16-QAM	$3\sqrt{2}$	10	20.61 dB	3.52 dB	17.09 dB
64-QAM	$7\sqrt{2}$	42	21.74 dB	4.65 dB	17.09 dB
256-QAM	$15\sqrt{2}$	170	22.29 dB	5.20 dB	17.09 dB

1) for all phase-shift keying (PSK) constellations, $A_{\max} = 1, \sigma_u^2 = 1, \mathrm{PAR}^{\mathrm{ofdm}} = N$, and $\mathrm{PAR}^{\mathrm{zp}} = P/N$;
2) for M-ary quadrature amplitude modulation (QAM) with $M = 2^{2n}, A_{\max} = (\sqrt{M}-1)\sqrt{2}, \sigma_u^2 = 2(M-1)/3$

$$\mathrm{PAR}^{\mathrm{ofdm}} = 3N \cdot \frac{\sqrt{M}-1}{\sqrt{M}+1}, \quad \mathrm{PAR}^{\mathrm{zp}} = \frac{3P}{N} \cdot \frac{\sqrt{M}-1}{\sqrt{M}+1}.$$

We list in Table I the PAR values (in decibels) for $N = 64, P = 80$, and different constellations $\mathcal{A}$. Notice that even for binary phase-shift keying (BPSK), the PAR can become as large as 18 dB for OFDM, while for ZP-only, it is only about 1 dB.

Although PAR is a meaningful parameter measuring the variation of the transmitted waveform in OFDM or ZP-only, it is rather pessimistic for OFDM. Indeed, although the peak power of a BPSK-modulated OFDM transmission increases linearly with the block size N, the probability that such a peak will occur decreases exponentially with N [32]. A more informative metric is the distribution of the instantaneous PAR.

By resorting to the central limit theorem (see, e.g., [51]), the components of $\tilde{\mathbf{u}}(i)$ can be shown (as $N \to \infty$) to be i.i.d. complex Gaussian with zero mean, and variance σ_u^2. The instantaneous PAR will then have a complementary probability distribution function given by

$$\Pr(\mathrm{PAR}_i^{\mathrm{ofdm}} > \gamma) = 1 - [1 - e^{-\gamma}]^N. \tag{10}$$

For ZP-only, the distribution of $\mathrm{PAR}_i^{\mathrm{zp}}$ depends on the constellation $\mathcal{A}$. For PSK constellations, $\|\mathbf{u}(i)\|_\infty^2 = 1, \mathrm{E}\|\mathbf{u}(i)\|^2 = N$, and therefore, $\mathrm{PAR}_i^{\mathrm{zp}} = P/N$. For M-QAM constellations and large M, we can approximate the discrete probability density function (pdf) of the encoded symbol $u(n)$ by a continuous density function given by

$$u(n) \sim \begin{cases} 1/\left(4A_{\max}^2\right), & \Re[u(n)] \le A_{\max}, \Im[u(n)] \le A_{\max} \\ 0, & \text{otherwise.} \end{cases} \tag{11}$$

With this approximation, it can be shown (see Appendix A) that the $|u(n)|$ follows the distribution shown in (12) at the bottom of the next page. The distribution of $\mathrm{PAR}_i^{\mathrm{zp}}$ is then given by (see also Appendix A)

$$\Pr\left(\mathrm{PAR}_i^{\mathrm{zp}} > \gamma\right) = 1 - \left[\Pr\left(|u(n)| \le \sqrt{\gamma N \bar{\sigma}_u^2/P}\right)\right]^N \tag{13}$$

where $\bar{\sigma}_u^2$ is the average energy per symbol computed according to the distribution in (11), and is found to be $\bar{\sigma}_u^2 = 2A_{\max}^2/3$. It is not difficult to see that the final distribution of $\mathrm{PAR}_i^{\mathrm{zp}}$ in (13) will not depend on $A_{\max}$, the actual size of the QAM constellation, as long as the constellation size is large enough.

In Fig. 2, we plot $\mathrm{PAR}_i^{\mathrm{ofdm}}$ of (10) and $\mathrm{PAR}_i^{\mathrm{zp}}$ of (13) for different constellations, together with numerical simulation results. The parameters are $N = 64$ and $P = 80$. As we can see,

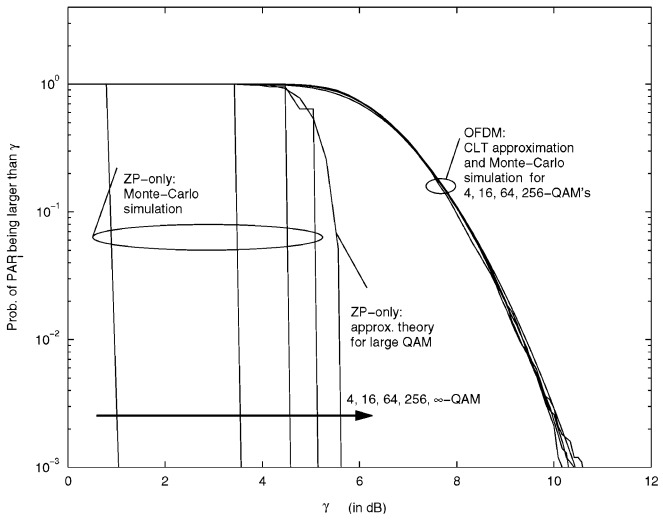

Fig. 2. Instantaneous PAR of OFDM versus ZP-only: approximation and simulation.

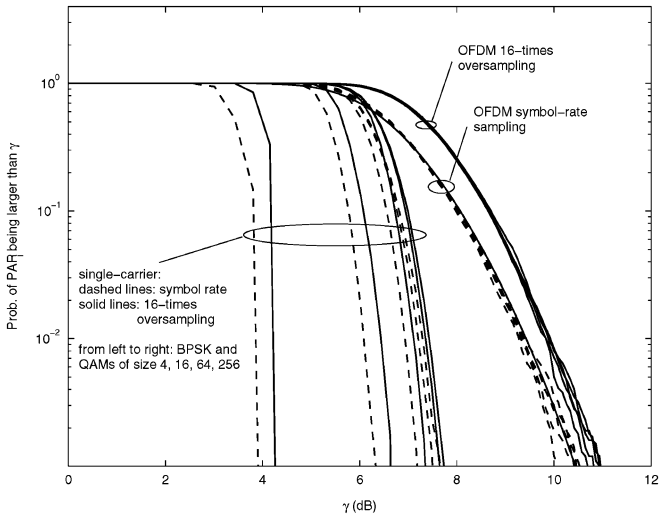

Fig. 3. Instantaneous PAR of continuous-time waveform: OFDM and ZP-only with square-root Nyquist pulse of roll-off factor 0.4.

the approximation (13) of ZP-only's instantaneous PAR for a large-size QAM is pessimistic, while the Gaussian approximation (10) by the central limit theory for OFDM is very accurate. If we fix the PAR outage probability, $\Pr(\mathrm{PAR}_i > \gamma) = 10^{-3}$, for both OFDM and ZP-only, the power amplifier for OFDM will require a 5.3–9.5-dB backoff as compared with that of ZP-only, depending on the constellation size. The effects of nonlinear distortion, and different power amplifier backoffs on the BER, have been studied, and also compared with single-carrier transmissions in [39]. Our analysis here quantifies analytically, and confirms the simulation-based observations of [39].

B. PAR of the Continuous-Time Signal With Non-Nyquist Pulses

For both OFDM and single-carrier transmissions, the PAR in the continuous waveform will depend on the spectral shaping pulse. For single-carrier transmissions, non-Nyquist spectral shaping pulses will increase the PAR of the transmitted continuous-time waveform relative to the one derived in Section III-A. We simulated the PAR of the continuous-time signal for a single-carrier ZP-only system with square-root raised-cosine spectral shaping pulse having rolloff factor 0.4. The results are depicted in Fig. 3, together with the PAR results for OFDM. We oversampled the continuous-time signal by a factor 16 to ensure that PAR values are close to those of the continuous-time signal. Symbol-rate sampled results are also shown as dashed lines. We can see that the continuous-time OFDM signal PAR is larger than the PAR of the symbol-rate sampled sequence in (10), by less than 1 dB. For single-carrier schemes, symbol-rate sampling and 16 times over sampling results are different by less than 0.5 dB. However, due to the fact that the spectral shaping pulse is not Nyquist (it is square-root Nyquist), ISI emerges, and renders the symbol-rate PAR larger than the Nyquist pulse case, by about 1–3 dB.

For more detailed studies of the PAR distribution in OFDM systems, the reader is referred to [14], [32], [52], and references therein. Many PAR-reduction techniques have been proposed, and their effects on the system capacity and performance have been studied, either in the frequency domain [6], [27], [34], [35], [43], or in the time domain (also known as clipping) [4], [12], [13], [21], [26], [33], [51].

Having discussed the PAR problem, we will assume in the sequel that the power amplifiers are linear and nonlinear distortions are absent. Such an assumption is optimistic, but enables us to simplify the analysis, and study other performance-determining factors separately.

IV. Sensitivity to CFO

Thanks to the orthogonality of the FFT basis, which is preserved when passing through frequency-selective channels, OFDM converts a frequency-selective channel into a set of flat-fading subchannels. However, the presence of CFO destroys the orthogonality among subcarriers. The FFT output at the receiver for each subcarrier will contain interfering terms from other subcarriers, the so-called intercarrier interference (ICI) effect. Another effect is the reduction of useful signal amplitude coming from power leakage to neighboring subcarriers.

For ZP-only, CFO acts like multiplicative noise that reduces the useful signal amplitude but does not cause ISI. For this reason, one would expect intuitively that ZP-only is more robust against CFO. In the following, we cite existing results on

$$\Pr(|u(n)| \le r) = \begin{cases} \pi r^2 / \left(4A_{\max}^2\right), & r \le (A_{\max}) \\ \left(\frac{\pi}{4} - \cos^{-1}\frac{A_{\max}}{r}\right)\frac{r^2}{A_{\max}^2} + \sqrt{\frac{r^2}{A_{\max}^2} - 1}, & A_{\max} < r \le \sqrt{2}A_{\max} \\ 1, & \text{otherwise} \end{cases} \tag{12}$$

the effect of signal-to-noise ratio (SNR), and analyze mutual information to benchmark the achievable transmission rate, when CFO is not compensated.

A. Degradation in SNR

When the CFO is small relative to the subcarrier spacing, the degradation for OFDM and single-carrier transmissions (ZP-only in this case) can be approximated, respectively, as [36]

$$\rho_{\rm snr}^{\rm ofdm} \approx \frac{10}{3\ln 10}(\pi f_o N)^2 \frac{E_s}{N_0} \text{ dB} \tag{14}$$

$$\rho_{\rm snr}^{\rm zp} \approx \frac{10}{3\ln 10}(\pi f_o)^2 \text{ dB} \tag{15}$$

where f_o is the normalized CFO, $f_o := f_{\rm off}/R_s$, with R_s denoting the symbol rate, and $f_{\rm off}$ the CFO in Hertz. We deduce from (14) and (15) that the degradation for both systems is proportional to the square of the CFO. For OFDM, the degradation is also proportional to the SNR, and the square of the number of subcarriers; the degradation for OFDM is $N^2 E_s/N_0$ times larger than that of ZP-only. The reason is that CFO introduces both ICI as well as reduction of the useful signal amplitude in OFDM, while ZP-only suffers only from the latter, which has a smaller effect than the former.

B. Effects on Mutual Information

We consider the average mutual information per block for random frequency-selective channels. Average mutual information is a meaningful measure for the achievable reliable transmission rate over ergodic channels, and has also been used in space–time communications [19], [42]. For notational brevity, we drop the block index i in this section only. We assume that: 1) only at the beginning of each received block, phase synchronization has been acquired; and 2) i.i.d. Gaussian symbols are transmitted in $\mathbf{u}(i)$.

With CFO present, we need to modify the OFDM model (3) as follows (see [39] for details):

$$\begin{aligned}\bar{\mathbf{x}} &= e^{j2\pi f_o(P-N)}\beta \mathbf{F}\mathbf{D}_o\tilde{\bar{\mathbf{H}}}\mathbf{F}^{\mathcal{H}}\bar{\mathbf{u}} + \boldsymbol{\eta} \\ &= e^{j2\pi f_o(P-N)}\beta \mathbf{F}\mathbf{D}_o\mathbf{F}^{\mathcal{H}}\mathbf{D}_H\bar{\mathbf{u}} + \boldsymbol{\eta}\end{aligned} \tag{16}$$

where $e^{j2\pi f_o(P-N)}$ is the phase shift of the $(L_{\rm cp}+1)$st symbol (the first noncyclic-prefixed symbol) caused by CFO, β is defined in (2), and $\mathbf{D}_o := \text{diag}[1, e^{j2\pi f_o}, \ldots, e^{j2\pi f_o(N-1)}]$. Suppose that the channel matrix $\mathbf{D}_H$ is known, while the CFO term $\mathbf{D}_o$ is unknown. Isolating the useful signal from interference and noise, we can rewrite (16) as

$$\bar{\mathbf{x}} = \beta\mathbf{D}_H\bar{\mathbf{u}} + \underbrace{\beta\mathbf{F}(e^{j2\pi f_o(P-N)}\mathbf{D}_o - \mathbf{I}_N)\mathbf{F}^{\mathcal{H}}\mathbf{D}_H\bar{\mathbf{u}} + \boldsymbol{\eta}}_{:=\mathbf{v}} \tag{17}$$

where $\mathbf{v}$ is Gaussian distributed (since $\bar{\mathbf{u}}$ and $\boldsymbol{\eta}$ are independent and Gaussian distributed), but statistically dependent on $\bar{\mathbf{u}}$. The dependence of $\mathbf{v}$ on $\bar{\mathbf{u}}$ offers information about $\bar{\mathbf{u}}$. With a fixed auto-covariance matrix for $\mathbf{v}$ in (17), the mutual information between $\bar{\mathbf{x}}$ and $\bar{\mathbf{u}}$ would be smallest if the noise term $\mathbf{v}$ and the information symbols $\bar{\mathbf{u}}$ are independent. For small CFO, the mutual information can then be well approximated and lower bounded as (see, e.g., ([10, (10.137)])

$$\mathcal{I}_{f_0}^{\rm ofdm}(\bar{\mathbf{x}};\bar{\mathbf{u}}) \gtrapprox \frac{1}{P}\text{E}_h\left[\log\det\left(\mathbf{I}_N + \mathbf{R}_{v\,|\,h}^{-1}\mathbf{D}_H\mathbf{D}_H^{\mathcal{H}}\right)\right] \tag{18}$$

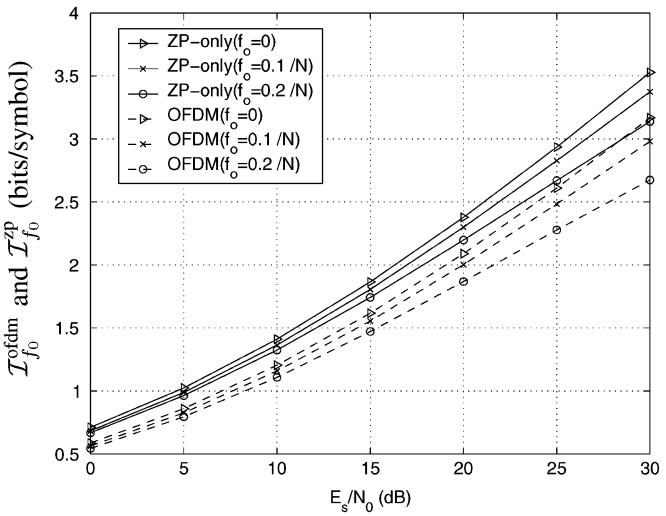

Fig. 4. Mutual information in the presence of CFO.

where $\mathbf{R}_{v\,|\,h} := \text{E}[\mathbf{v}\mathbf{v}^{\mathcal{H}}] = \sigma_\eta^2\mathbf{I}_N + E_s\beta^2\mathbf{F}(e^{j2\pi f_o(P-N)}\mathbf{D}_o - \mathbf{I}_N)\mathbf{F}^{\mathcal{H}}\mathbf{D}_H\mathbf{D}_H^{\mathcal{H}}\mathbf{F}(e^{-j2\pi f_o(P-N)}\mathbf{D}_o^{\mathcal{H}} - \mathbf{I}_N)\mathbf{F}^{\mathcal{H}}$, and the expectation in (18) is with respect to the symbols and the noise, for a given channel. The lower bound offers a close approximation, especially for small CFO, where the statistical dependence between $\mathbf{v}$ and $\bar{\mathbf{u}}$ is small.

For ZP-only, we have the following input–output relationship when CFO is present:

$$\mathbf{y} = \bar{\mathbf{D}}_o\bar{\mathbf{H}}\bar{\mathbf{u}} + \boldsymbol{\zeta} = \bar{\mathbf{H}}\bar{\mathbf{u}} + (\bar{\mathbf{D}}_o - \mathbf{I}_P)\bar{\mathbf{H}}\bar{\mathbf{u}} + \boldsymbol{\zeta}. \tag{19}$$

where $\bar{\mathbf{D}}_o := \text{diag}[1, e^{j2\pi f_o}, \ldots, e^{j2\pi f_o(P-1)}]$.

Define now $\mathbf{w} := (\bar{\mathbf{D}}_o - \mathbf{I}_P)\bar{\mathbf{H}}\bar{\mathbf{u}} + \boldsymbol{\zeta}$, which is Gaussian, but dependent on $\mathbf{u}$. Similar to OFDM, the mutual information for ZP-only can be well approximated, and lower bounded by (see, e.g., [10, (10.137)]):

$$\mathcal{I}_{f_0}^{\rm zp}(\mathbf{y};\bar{\mathbf{u}}) \gtrapprox \frac{1}{P}\text{E}_h\left[\log\det\left(\mathbf{I}_P + E_s\mathbf{R}_{w\,|\,h}^{-1}\bar{\mathbf{H}}\bar{\mathbf{H}}^{\mathcal{H}}\right)\right] \tag{20}$$

where

$$\mathbf{R}_{w\,|\,h} := \text{E}[\mathbf{w}\mathbf{w}^{\mathcal{H}}] = \sigma_\zeta^2\mathbf{I}_P + E_s(\bar{\mathbf{D}}_o - \mathbf{I}_P)\bar{\mathbf{H}}\bar{\mathbf{H}}^{\mathcal{H}}(\bar{\mathbf{D}}_o - \mathbf{I}_P)^{\mathcal{H}}.$$

Expressions in (18) and (20) are valid for a single fixed CFO. If f_o is random with pdf $\text{P}(f_o)$, then $\mathcal{I}_{f_0}^{\rm ofdm}(\bar{\mathbf{x}};\bar{\mathbf{u}})$ and $\mathcal{I}_{f_0}^{\rm zp}(\mathbf{y};\bar{\mathbf{u}})$ should be computed as the expectation of the expressions in (18) and (20) with respect to $\text{P}(f_o)$.

To compare both systems in the presence of CFO, we depict in Fig. 4 the mutual information as given by (18) and (20) with $(N, L_{\rm cp}, P) = (64, 16, 80)$. The channel consists of six zero-mean complex Gaussian i.i.d. taps, each of variance $1/6$. The mutual information is not appreciably affected by the CFO. When the offset is 20% of the carrier spacing, the capacity loss is about 0.3 b/symbol at 20 dB for both OFDM and ZP-only. However, we notice that with or without CFO, the ZP-only achieves higher mutual information than OFDM, which is partly due to the power loss in OFDM by inserting CP.

When mobility induces Doppler spread, the channel is time varying, and the analysis becomes more difficult. SNR degradation in the presence of Doppler is studied in [38], together with the BER floor caused by ICI. Nevertheless, viewing Doppler effect as the superposition of *multiple* CFOs, we expect ZP-only

to be more robust to Doppler effects than OFDM, based on our comparison in the presence of a *single* CFO.

V. Uncoded System Performance and Complexity

In this section, we will compare uncoded OFDM with uncoded ZP-only. Since there is no encoding at the transmitter, we have just for this section $\mathbf{u}(i) = \mathbf{s}(i)$. That is, we assume that the symbols in $\mathbf{u}(i)$ are i.i.d. with zero-mean and variance σ_u^2. We will examine the performance of various block equalizers, including ZF linear equalizer (ZF-LE), MMSE-LE, as well as nonlinear decision-feedback equalizers (MMSE-DFE), and maximum-likelihood (ML) decoders. In all our simulations in this and the next sections, we use BPSK constellations for both OFDM (without any PAR compensation) and single-carrier schemes.

A. Uncoded OFDM

For the uncoded OFDM in (3), an $N \times N$ matrix $\mathbf{G}$ can be used to describe a linear block equalizer that yields $\hat{\mathbf{u}}(i) = \mathbf{G}\mathbf{x}(i)$. ZF and MMSE equalizers can be written, respectively, as

$$\mathbf{G}_{\rm zf}^{\rm ofdm} = \frac{1}{\beta}\mathbf{D}_H^{\dagger} \tag{21}$$

$$\mathbf{G}_{\rm mmse}^{\rm ofdm} = \beta\sigma_u^2\mathbf{D}_H^{\mathcal{H}}\left(\sigma_\eta^2\mathbf{I}_N + \beta^2\sigma_u^2\mathbf{D}_H\mathbf{D}_H^{\mathcal{H}}\right)^{-1}. \tag{22}$$

For the MMSE equalizer, the autocorrelation matrix of the estimation error, $\mathbf{e}(i) := \mathbf{u}(i) - \hat{\mathbf{u}}(i)$, can be found to be $\mathbf{R}_{\rm ee,mmse}^{\rm ofdm} = (\sigma_u^{-2}\mathbf{I}_N + \sigma_\eta^{-2}\beta^2\mathbf{D}_H^{\mathcal{H}}\mathbf{D}_H)^{-1}$.

Since $\mathbf{D}_H$ is diagonal, both $\mathbf{G}_{\rm zp}^{\rm ofdm}$ and $\mathbf{G}_{\rm mmse}^{\rm ofdm}$ are diagonal, implying per-subcarrier equalization simplicity. Given the channel, $\mathcal{O}(N)$ computations are needed to calculate these equalizers in (21), and only $\mathcal{O}(N)$ computations are required to detect symbol estimates using $\hat{\mathbf{u}}(i) = \mathbf{G}\mathbf{x}(i)$, possibly followed by appropriate quantization (hard decision). If we also count the $\mathcal{O}(N\log N)$ computations needed for the FFT, only $\mathcal{O}(\log N)$ computations are needed per symbol, which is one of the major advantages of OFDM.

But the disadvantage here is the loss of symbol detectability. If the channel happens to have a null on (or close to) one of the FFT subcarriers, $\{\exp(-j2\pi n/N)\}_{n=0}^{N-1}$, the matrix $\mathbf{D}_H$ will become singular (or ill conditioned), and the corresponding symbol carried by that frequency will be impossible to detect even if the noise is absent. In other words, there exist "bad" channels that can render symbol detection impossible. Such a lack of symbol detectability is closely related to the loss of diversity when the channel exhibits frequency-selective fading. In fact, it can be shown that uncoded OFDM has diversity order of only one, see, e.g., [5], [45], and [46]. The diversity order determines the slope of the probability of error versus SNR curve in a log-log scale at high SNR.

Since $\boldsymbol{\eta}(i)$ is AWGN, and $\mathbf{D}_H$ is diagonal, the ML detection of each symbol in $\mathbf{u}(i)$ is independent of other symbols. In fact, the ML estimator is just the ZF equalizer in (21), followed by an appropriate minimum-distance quantizer that depends on the constellation used. Thus, the ZF equalizer in OFDM in general outperforms the MMSE equalizer in BER, although the latter offers lower MSE. Because of the independent parallel channel structure of OFDM, there is no need for a decision-aided detector that passes past decisions across subcarriers.

When the symbols are BPSK, the BER with ML equalization is computable in closed form as

$$\mathrm{BER}_{\rm ml,BPSK}^{\rm ofdm} = \frac{1}{N}\sum_{i=0}^{N-1} Q\left(\frac{\beta|H(e^{j2\pi i/N})|\sigma_u}{\sigma_\eta}\right) \overset{N\to\infty}{\longrightarrow} \int_0^1 Q \times \left(\frac{\beta|H(e^{j2\pi f})|\sigma_u}{\sigma_\eta}\right) df \tag{23}$$

where $Q(x) := \int_x^\infty (2\pi)^{-1/2}\exp(-x^2/2)dx$. When the channel taps are complex Gaussian distributed, $|H(e^{j2\pi f})|$ is Rayleigh distributed for all f. When averaged over channel realizations, the channel-dependent performance (23) will give diversity order one; see, e.g., [49].

B. Uncoded ZP-Only

For ZP-only, various equalizers are available. Based on the model in (4), a fat $N \times P$ matrix $\mathbf{G}^{\rm zp}$ can be used as a linear block equalizer to yield $\hat{\mathbf{u}}(i) = \mathbf{G}^{\rm zp}\mathbf{y}(i)$. Its ZF and MMSE versions can be written, respectively, as

$$\mathbf{G}_{\rm zf}^{\rm zp} = \mathbf{H}^{\dagger} \quad \text{and} \quad \mathbf{G}_{\rm mmse}^{\rm zp} = \sigma_u^2\mathbf{H}^{\mathcal{H}}\left(\sigma_\eta^2\mathbf{I}_P + \sigma_u^2\mathbf{H}\mathbf{H}^{\mathcal{H}}\right)^{-1}. \tag{24}$$

For the MMSE equalizer, the autocorrelation matrix of the estimation error $\mathbf{e}(i) := \mathbf{u}(i) - \hat{\mathbf{u}}(i)$ can be found to be $\mathbf{R}_{\rm ee,mmse}^{\rm zp} = (\sigma_u^{-2}\mathbf{I}_N + \sigma_\eta^{-2}\mathbf{H}^{\mathcal{H}}\mathbf{H})^{-1}$. Notice that because of the Toeplitz convolution matrix $\mathbf{H}$, the ZF equalizer $\mathbf{G}_{\rm zf}^{\rm zp}$ in (24) always exists, which implies that the transmitted uncoded symbols are *always detectable* when the noise is sufficiently small. This is to be contrasted with uncoded OFDM, which does not guarantee symbol detectability. Complexity-wise, the matrix inversions in (24) can be performed with $\mathcal{O}(N^2)$ flops using Schur-type methods [28], [29], thanks to the Toeplitz structure of the matrix involved (it is easy to verify that both $\mathbf{H}^{\mathcal{H}}\mathbf{H}$ and $\mathbf{H}\mathbf{H}^{\mathcal{H}}$ are Toeplitz). The subsequent matrix-vector product for obtaining $\hat{\mathbf{u}}(i)$ will take no more than $\mathcal{O}(N^2)$ flops per block. So, the complexity per symbol of such linear block equalizers is $\mathcal{O}(N)$.

If BPSK symbols are used, then the average BER and its limit as $N \to \infty$ are given by

$$\mathrm{BER}_{\rm zf}^{\rm zp} = \frac{1}{N}\sum_{n=0}^{N-1} Q\left(\frac{\sigma_u}{\sigma_\eta\sqrt{[(\mathbf{H}^{\mathcal{H}}\mathbf{H})^{-1}]_{k,k}}}\right) \overset{N\to\infty}{\longrightarrow} Q \times \left(\frac{\sigma_u}{\sigma_\eta\left(\int_0^1 |H(e^{j2\pi f})|^{-2}\,df\right)^{1/2}}\right) \tag{25}$$

where the limiting form can be obtained by noticing that as $N \to \infty, \mathbf{H}$ becomes approximately circulant and thus diagonalizable by (I)FFT matrices. The term $[(\mathbf{H}^{\mathcal{H}}\mathbf{H})^{-1}]_{k,k}$ becomes asymptotically identical for all k's, which means that the symbols will have equal probability of error as $N \to \infty$. This is not the case with OFDM.

At high SNR, performance of MMSE approaches that of ZF equalization. It is also possible to use block DFE for uncoded ZP-only, which is free of IBI because of the ZP guard. As a result, the detection of different blocks can be separated without

affecting performance. The DFE relies on the $N \times P$ feed-forward matrix $\mathbf{W}$ and the $N \times N$ matrix $\mathbf{B}$ to pass past symbol decisions *within* one block. Since a decision has to be made before it can be fed back, matrix $\mathbf{B}$ is required to be lower or upper triangular, depending on whether the first or the last symbol in a block $\mathbf{u}(i)$ is decided first.

Matrices $\mathbf{W}$ and $\mathbf{B}$ can be designed so that the MSE between the estimated block *before* the decision device is minimized. When the last symbol in $\mathbf{u}(i)$ is decided first, $\mathbf{B}$ is upper triangular. The filtering matrices $\mathbf{W}$ and $\mathbf{B}$ can be found from the following equations (see also [41]):

$$\begin{cases} \sigma_u^{-2}\mathbf{I}_N + \sigma_\eta^{-2}\mathbf{H}^{\mathcal{H}}\mathbf{H} = \mathbf{U}^{\mathcal{H}}\mathbf{\Lambda}\mathbf{U} \\ \mathbf{W} = \mathbf{U}\mathbf{G}_{\text{mmse}}^{\text{zp}}, \qquad\qquad \mathbf{B} = \mathbf{U} - \mathbf{I} \end{cases} \tag{26}$$

where $\mathbf{G}_{\text{mmse}}^{\text{zp}}$ is as in (24), and $\mathbf{U}$ is an upper triangular matrix with unit diagonal entries, obtained using Cholesky's decomposition [2], [8], [41]. Cholesky decomposition of the Toeplitz matrix $\sigma_u^{-2}\mathbf{I}_N + \sigma_\eta^{-2}\mathbf{H}^{\mathcal{H}}\mathbf{H}$, requires $\mathcal{O}(N^2)$ flops using Schur-type algorithms [28], [29]. With the filtering operations $\mathcal{O}(N^2)$ per block counted, the block MMSE-DFE has a per-symbol complexity of order $\mathcal{O}(N)$. Notice that although the block MMSE-DFE is presented in matrix form, the symbol decision feedback is conducted in a serial form, as indicated by the triangular structure of $\mathbf{B}$.

It can be shown that if we ignore error propagation, then the autocorrelation matrix of the error $\mathbf{e}(i) := \mathbf{u}(i) - \hat{\mathbf{u}}(i)$ is $\mathbf{R}_{\text{ee,dfe}}^{\text{zp}} = \mathbf{\Lambda}^{-1}$ (e.g., [41]). Furthermore, it can be shown that $[\mathbf{R}_{\text{ee,dfe}}^{\text{zp}}]_{n,n} \leq [\mathbf{R}_{\text{ee,mmse}}^{\text{zp}}]_{n,n}$, for $n \in [0, N-1]$. Thus, if we do not consider the effect of error propagation, block MMSE-DFE will have smaller MSE than the linear MMSE equalizer in (24).

Compared with *serial* transmissions with DFE (e.g., [23]), one major advantage of ZP block transmissions is that they allow decisions to be made within a block, and hence, prevent error propagation from block to block. Alternatively, we can view the padded zeros as symbols that have been perfectly decided, and thus contain no error; these symbols, in essence, "reset" the DFE to a known all-zero state.

When the symbols in $\mathbf{u}(i)$ are complex with independent real and imaginary parts, we could also apply a block MMSE-DFE to detect $\Re\{\mathbf{u}(i)\}$ and $\Im\{\mathbf{u}(i)\}$ separately, based on

$$\begin{bmatrix} \Re\{\mathbf{y}(i)\} \\ \Im\{\mathbf{y}(i)\} \end{bmatrix} = \begin{bmatrix} \Re\{\mathbf{H}\} & -\Im\{\mathbf{H}\} \\ \Im\{\mathbf{H}\} & \Re\{\mathbf{H}\} \end{bmatrix} \begin{bmatrix} \Re\{\mathbf{u}(i)\} \\ \Im\{\mathbf{u}(i)\} \end{bmatrix} + \begin{bmatrix} \Re\{\boldsymbol{\xi}(i)\} \\ \Im\{\boldsymbol{\xi}(i)\} \end{bmatrix}.$$

Such a model doubles the problem size as compared to the complex signal model in (4), but it enables detection of the real and imaginary parts separately. Hence, when, for instance, the real part is detected first, the decision can be fed back to facilitate detection of the imaginary part. Theoretically, such a model leads to lower symbol-error estimates when the effect of decision errors is neglected, and we will use it in our simulations.

For ZP-only, it is also possible to perform ML equalization. Because of the banded structure of the convolution matrix $\mathbf{H}$ [cf. (4)], or the Markovian property of the channel input–output relationship, we can apply the VA [18]. The complexity of ML decoding is $\mathcal{O}(M^L)$ per symbol, or $\mathcal{O}(NM^L)$ per block, where M is the constellation size. The ML equalizer will thus be practical only when M and/or L are relatively small. Other detections algorithms that can be applied to ZP-only include the sphere-decoding algorithm and the BLAST nulling-canceling algorithm, see, e.g., [24], [25], and [50].

TABLE II
PER-SYMBOL COMPLEXITY OF VARIOUS EQUALIZERS

	ZF	Linear MMSE	MMSE-DFE	ML
OFDM	$\mathcal{O}(\log N)$	$\mathcal{O}(\log N)$	–	$\mathcal{O}(\log N)$
ZP-only	$\mathcal{O}(N)$	$\mathcal{O}(N)$	$\mathcal{O}(N)$	$\mathcal{O}(M^L)$

Performance analysis of ZP-only block transmissions with ML equalization is complicated. But the upper bounds that have been derived for serial transmissions over ISI channels are applicable here, too [18]. For a fixed channel, the BER can be well approximated and upper bounded by $\text{BER}_{\text{ml}}^{\text{zp}}(h) \approx K_1 Q(d_{\min}/2\sigma_\eta)$, where K_1 is a constant depending on the constellation, and $d_{\min}$ is the minimum Euclidean distance between two possible received blocks, i.e., $d_{\min} = \min |\mathbf{Hu}(i) - \mathbf{Hu}'(i)|$, $\mathbf{u}(i) \neq \mathbf{u}'(i)$. A flow-graph method can be used to determine $d_{\min}$ for a given channel (see, e.g., [18]).

If the channel is time varying but remains approximately constant over one block, we can model it as consisting of random coefficients. Using the pairwise error probability (PEP) analysis of [45], the average probability of error can be well approximated by

$$\overline{\text{BER}_{\text{ml}}^{\text{zp}}} := \text{E}_h\left\{\text{BER}_{\text{ml}}^{\text{zp}}(h)\right\} \approx \left(G_c \frac{E_s}{N_0}\right)^{-G_d}$$

where G_d is a constant determining the slope of the BER-SNR curve, and is, therefore, called *diversity order*; while G_c is another constant determining the savings in SNR, as compared with a $(E_s/N_0)^{-G_d}$ curve, and is thus called *coding gain*. The coding gain often measures performance of coded transmissions, but is also appropriate here for describing uncoded system performance. Uncoded ZP-only will turn out to enjoy great advantages in terms of diversity order and coding gain, as we will show in the next subsection.

C. Complexity, Diversity, and Coding Gain Comparisons

To compare uncoded OFDM with ZP-only on the basis of receiver complexity, we tabulate the approximate number of flops needed for each of the various equalization alternatives in Table II. ZP-only has higher complexity than OFDM, especially when ML detection is used. But at the price of complexity, ZP-only, in general, offers considerably improved performance with random channels, thanks to its enhanced diversity and coding gains.

To establish the superiority of uncoded ZP-only performance in terms of diversity order and coding gain, we consider a general class of transmission schemes that we call linearly precoded (LP) OFDM [45]. This class includes not only multicarrier, but also single-carrier block transmissions. Specifically, instead of encoding $\mathbf{s}(i)$ using Galois field coding, we linearly precode it using the $N \times K$ matrix $\mathbf{\Theta}$ to yield $\mathbf{u}(i) = \mathbf{\Theta}\mathbf{s}(i)$, which is then

transmitted using OFDM. Replacing $\mathbf{u}(i)$ in (3) by $\mathbf{\Theta s}(i)$, we obtain the MIMO model

$$\mathbf{x}(i) = \beta \mathbf{D}_H \mathbf{\Theta s}(i) + \boldsymbol{\eta}(i). \tag{27}$$

In general, we require $\mathbf{\Theta}$ to be square or tall ($N \geq K$), but here the LP class will also include fat precoders ($N < K$). We impose the constraint $\mathrm{tr}(\mathbf{\Theta}^{\mathcal{H}}\mathbf{\Theta}) = K$, so that LP does not change the energy per symbol in $\mathbf{s}(i)$. Both OFDM and ZP-only belong to this class of LP block transmissions. Indeed, setting $K = N$ and $\mathbf{\Theta} = \mathbf{I}_N$, we have the uncoded OFDM. Interestingly, setting $K = N - L_{\mathrm{zp}}$, and $\mathbf{\Theta}$ to be the first K columns of an $N \times N$ FFT matrix, that is, $[\mathbf{\Theta}]_{n,k} = \exp(-j2\pi nk/N)$, we obtain a ZP-only system. The reason is that at the OFDM transmitter, the IFFT matrix $\mathbf{F}^{\mathcal{H}}$ and $\mathbf{\Theta}$ partly annihilate each other, as $\mathbf{F}^{\mathcal{H}}\mathbf{\Theta} = [\mathbf{I}_K \mathbf{0}_{K\times L_{\mathrm{zp}}}]^T$, where $\mathbf{0}_{K\times L_{\mathrm{zp}}}$ is an all-zero matrix. What $[\mathbf{I}_K \mathbf{0}_{K\times L_{\mathrm{zp}}}]^T$ does on $\mathbf{s}(i)$ is just padding it with $L_{\mathrm{zp}} = L_{\mathrm{cp}}$ zeros. Cyclic-prefixing OFDM now becomes unnecessary because it prepends each block $\mathbf{u}(i)$ with a repetition of the padded L_{zp} zeros, and the result is that two successive blocks are now separated by $2L_{\mathrm{cp}}$ zeros, more than the necessary upper bound L_{cp} on the channel order. Eliminating CP in this case will give us an uncoded ZP-only system with its information block size K and ZP block size N, which is different from the uncoded ZP-only system in the previous parts of this section with regards to the information block size. Notice also that we no longer need the power loss factor β, since a CP has not been inserted.

We will see that all ZP transmissions have the same maximum diversity order and maximum coding gain among the class of LP-OFDM, irrespective of their block size. Specifically, we have the following result that we prove in Appendix B.

Theorem 1: Consider an LP-OFDM system as in (27), where the entries of $\mathbf{s}(i)$ are drawn independently from a finite alphabet set $\mathcal{A} \subset \mathbb{C}$, and let $\mathbf{R}_h$ denote the autocorrelation matrix of the Rayleigh channel $\mathbf{h} := [h(0), \ldots, h(L)]^T$. Then the maximum diversity order for an LP-OFDM system with $N \geq L_{\mathrm{cp}}$ is $G_{\mathrm{d,max}} = \mathrm{rank}(\mathbf{R}_h)$, which is achieved by ZP-only transmissions. If $\mathbf{R}_h$ has full rank $L+1$, then the maximum coding gain of LP-OFDM is $G_{c,\max} = [d^2_{\min,\mathcal{A}} \det^{(1/(L+1))}(\mathbf{R}_h)/\mathcal{E}_{s,\mathcal{A}}]$, where $d_{\min,\mathcal{A}} = \min\{|a_1 - a_2| \,|\, a_1, a_2 \in \mathcal{A}, a_1 \neq a_2\}$, and $\mathcal{E}_{s,\mathcal{A}}$ is the average symbol energy in $\mathcal{A}$. The maximum coding gain is achieved by ZP-only transmissions.

To show the difference in performance, we depict in Fig. 5 the BER/SNR curves of various equalizers with parameters $(N, L, P) = (64, 2, 66)$. The channel is of length $L + 1 = 3$, with i.i.d. taps of variance $1/3$. BPSK constellation is used. CP length $L_{\mathrm{cp}} = 16$, mimicking the setup in HIPERLAN/2. From the slope of the ML curves, we deduce that uncoded OFDM has only diversity 1, while ZP-only approximately has diversity 3. For ZP-only, the block MMSE-DFE performs only slightly worse than the ML equalizer.

When the portion of ZP becomes small compared with the block size, ZP-only behaves like an SSC transmission. To show this, we compare the performance of ZP-only with SSC transmissions in Fig. 6, with parameters $(N, L, P) = (64, 10, 74)$, over random Rayleigh fading channels. Block MMSE-DFE for ZP-only and serial MMSE-DFE for SSC transmissions perform

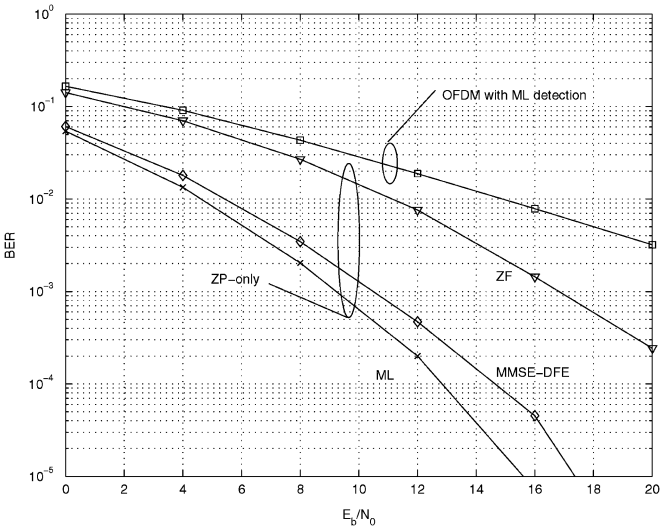

Fig. 5. Performance of uncoded OFDM versus ZP-only.

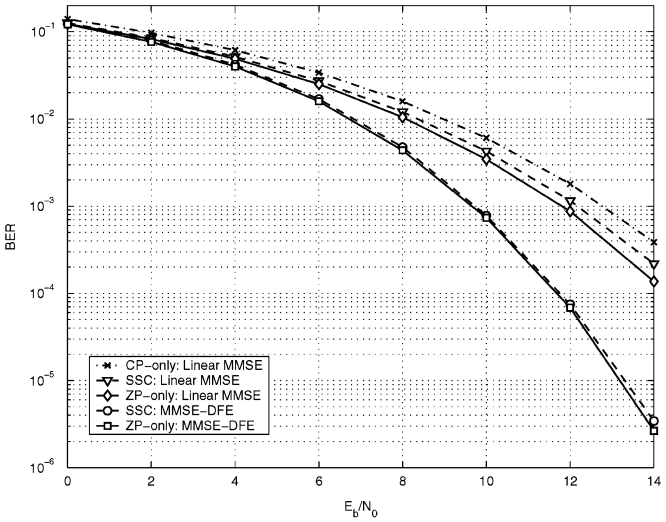

Fig. 6. Performance of ZP-only, SSC transmissions, and CP-only.

almost identically. The block linear MMSE-DEF for ZP-only performs slightly better than serial MMSE-DFE for SSC transmissions. These comparisons show that the error-rate performance results for ZP-only can also be applied to SSC transmissions, provided that ZP guard occupies a small portion of each transmitted block. Also shown in Fig. 6 is the linear MMSE performance of a CP extended single-carrier transmission (labeled CP-only) proposed for low-complexity frequency-domain equalization in [9] and [39]. There is a performance loss of about 0.5 dB, as compared with SSC transmissions without CP or ZP, due to the energy waste caused by the CP guard.

VI. Coded System Performance and Complexity

We have seen that uncoded OFDM is inferior to uncoded ZP-only system, although uncoded OFDM offers low equalization complexity. In this section, we compare convolutionally coded OFDM with a coded ZP-only system. Because accurate analysis is difficult, the performance comparison will be conducted mainly by simulation.

A. Decoding Algorithm

For decoding coded OFDM transmissions, we adopt the VA as described in, e.g., [18], [31], and [39]. Compared with decoding of serial coded transmissions over an AWGN channel, we need to slightly modify the path metric computations. Specifically, if we are to decode a total of I transmitted blocks, then we can write the path log-likelihood function based on the parallel channel model of (3) as follows:

$$\log \Pr\left(\{\mathbf{x}(i)\}_{i=0}^{I-1} \middle| \{\mathbf{u}(i)\}_{i=0}^{I-1}\right) = -\frac{1}{2\sigma_\eta^2}\sum_{i=0}^{I-1}\sum_{n=0}^{N-1}[|[\mathbf{x}(i)]_n - \beta H(e^{j2\pi n/N})[\mathbf{u}(i)]_n|^2 - NI\log(\sqrt{2\pi}\sigma_\eta)]$$

which differs from the AWGN case only in the scalars $\beta H(e^{j2\pi f})$.

For convolutionally coded ZP-only, ML detection of the information symbols can be achieved by treating the convolutional channel as a convolutional encoder, and thereby jointly decoding the channel and the convolutional code using the Viterbi decoder. The complexity, however, will be exponential in the sum of the channel order and the convolutional code memory, which can often be prohibitively large.

Suboptimal decoders split the detection process in two parts, channel equalization followed by convolutional decoding. In the equalization step, the coded symbols are treated as i.i.d., which leads to the suboptimality. Any of the equalizers in Section V-B can be used. But for lower complexity relative to the ML decoder, and better performance, compared with the linear equalizers, we advocate the usage of block MMSE-DFE.

Using MMSE-DFE, we first obtain estimates $\{\hat{\mathbf{u}}(i)\}_{i=0}^{I-1}$ of I blocks of coded symbols. These estimates are then passed on to a Viterbi processor to decode $\{\mathbf{s}(i)\}_{i=0}^{I-1}$. The estimates $\{\hat{\mathbf{u}}(i)\}_{i=0}^{I-1}$ are fed to the Viterbi decoder in *soft* form, that is, before they are quantized by the decision device (hard decisions are still made for the feedback loop in the DFE). As we mentioned in Section V-B, the symbol-error autocorrelation matrix in MMSE-DFE is given by $\mathbf{R}_{\text{ee,dfe}}^{\text{zp}} = \mathbf{\Lambda}^{-1}$, implying that symbol-error estimates are uncorrelated if we neglect the effects of error propagation. If we further approximate the symbol-error estimates, which consist of noise and residual ISI, as Gaussian distributed, then they become independent. Let us define $\mathbf{z}(i) := \sigma_\eta \mathbf{\Lambda}^{(1/2)}\hat{\mathbf{u}}(i)$, and rewrite it as

$$\mathbf{z}(i) \approx \sigma_\eta \mathbf{\Lambda}^{(1/2)}\mathbf{u}(i) + \boldsymbol{\zeta}(i) \tag{28}$$

where $\boldsymbol{\zeta}(i)$ is AWGN having i.i.d. entries with variance σ_η^2. Comparing (28) with (3), we notice that under the assumptions that we have made (i.e., no error propagation and Gaussian errors) MMSE-DFE also converts the ISI channel into parallel independent subchannels with additive noise of variance σ_η^2. The parallel channel is $\beta\mathbf{D}_H$ in OFDM, and $\sigma_\eta\mathbf{\Lambda}^{(1/2)}$ in ZP-only with block MMSE-DFE. Obviously, the distribution of the diagonal entries in $\beta\mathbf{D}_H$ and $\sigma_\eta\mathbf{\Lambda}^{(1/2)}$ will affect differently the performance of the two systems in both coded and uncoded cases.

With MMSE-DFE and the model in (28), the same VA used in coded OFDM can be applied to coded ZP-only. As far as complexity is concerned, the ZP-only has to implement an extra MMSE-DFE, which incurs complexity $\mathcal{O}(N)$ per symbol. When N is comparable to the number of states in the convolutional code trellis, as in the HIPERLAN/2 setup, the extra complexity of ZP-only will be of the same order as in the VA, which will make the coded ZP-only have comparable complexity with coded OFDM. We also remark that as with serial MMSE-DFE [7], the soft output of the block MMSE-DFE is biased. This motivates usage of an unbiased MMSE-DFE that properly scales the equalizer output to achieve a lower probability of error.

TABLE III
CHANNEL MODELS FOR HIPERLAN/2 CODED SYSTEMS

tap index	Model A	Model B	tap index	Model A	Model B
0	4.51e-01	2.60e-01	8	3.87e-04	1.07e-02
1	3.47e-01	2.44e-01	9	0	6.45e-03
2	1.28e-01	2.24e-01	10	0	5.01e-03
3	5.22e-02	7.07e-02	11	0	2.51e-03
4	1.02e-02	7.93e-02	12	0	0
5	7.72e-03	4.78e-02	13	0	1.48e-03
6	2.87e-03	2.95e-02	14	0	0
7	1.04e-03	1.78e-02	15	0	6.02e-04

B. Simulation Results

We use simulation to compare the performance of both systems with coding. We will use the convolutional code specified in the HIPERLAN/2 standard [16]. The mother code has constraint length of seven and rate $1/2$. The trellis for this code has $2^6 = 64$ states, which happens to be the same as the total number of subcarriers. There are 16 subcarriers in the HIPERLAN/2 standard that are null, or serve as pilot tones. So, the number of information-bearing symbols per block is $N = 48$. After encoding, the coded symbols are grouped, interleaved, and mapped to a given constellation, as detailed in [16]. We only consider quaternary phase-shift keying (QPSK) here. After the constellation symbol blocks are formed, they are transmitted either using an OFDM or a ZP-only system. The symbols corresponding to null subcarriers in OFDM are set to zero in ZP-only to maintain the same rate for both systems. The rate-$1/2$ code with QPSK provides a nominal bit rate of 12 Mb/s in the HIPERLAN/2 setup. A bit rate of 18 Mb/s is achieved by puncturing the coded symbols before interleaving, using the puncturing pattern (1, 1, 1, 0, 0, 1) to a code rate of $3/4$, as specified in the standard.

The channel models we consider here are slightly modified versions of those specified in [15]. We use Model A and Model B in the simulations, where Model A corresponds to a typical office environment, and Model B corresponds to a typical large open space environment with nonline-of-sight conditions, or an office environment with large delay spread. The modification we made was to round each tap, as given in the standard, to the nearest symbol-rate sampled discrete-time equivalent channel tap. The resulting models will still be called A and B for convenience. Their taps are independent complex Gaussian random variables with variances given in Table III. The variances are normalized such that the total variance is one.

We depict the simulation results in Fig. 7 for rate $1/2$, and in Fig. 8 for rate $3/4$. The BER performance is averaged over 200

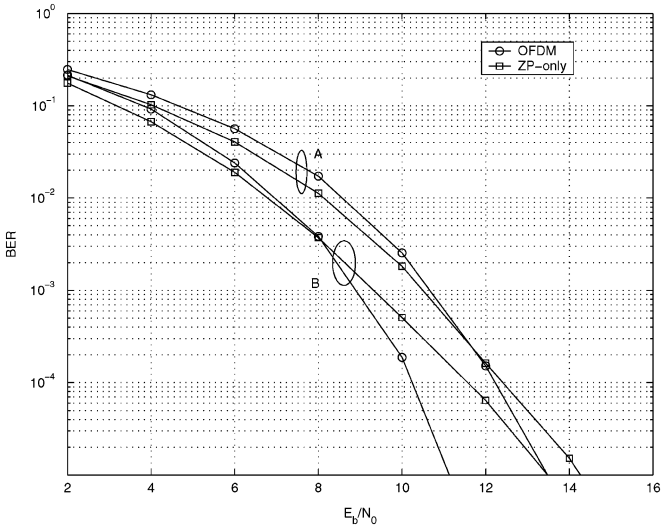

Fig. 7. Performance of coded OFDM versus ZP-only: rate $1/2$.

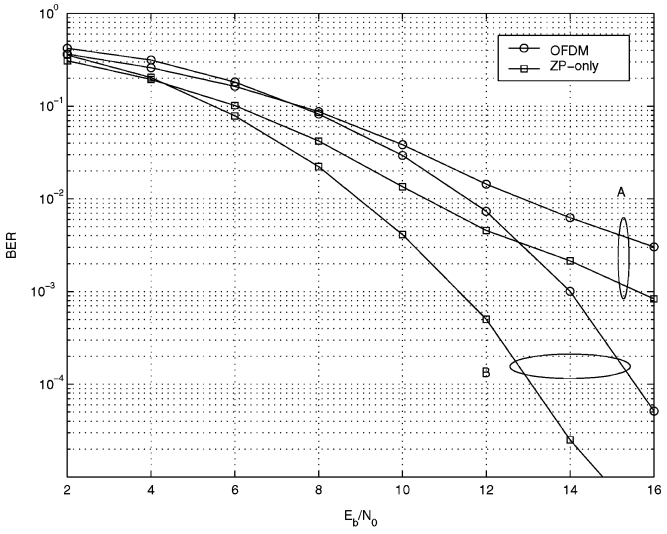

Fig. 8. Performance of coded OFDM and ZP-only: rate $3/4$.

randomly generated channels. We can see that in the rate-$1/2$ case, OFDM outperforms ZP-only at high SNR (8 dB for channel B and 12 dB for channel A). For channel B, OFDM has an advantage of about 2 dB in SNR over ZP-only. The main reason behind ZP-only's inferiority is due to its suboptimality in decoding caused by three effects: error propagation, non-Gaussianity of the error, and non-ML decisions in the DFE. These effects could be overcome if we use a turbo-like iteration and combined equalization with decoding. Preliminary results on these iterative equalization/decoding alternatives can be found in [47].

The situation changes with rate $3/4$ case. For both channel A and channel B, coded ZP-only exhibits at least a 2-dB advantage in SNR. The reason is that uncoded ZP-only already enjoys full diversity and coding gains, while the rate-$3/4$ error-control code is mainly used to cope with residual ISI and additive noise. In contrast, the uncoded OFDM system has diversity order of one, and the relatively "weak" error-control code undertakes the task of not only improving over OFDM's poor diversity, but also

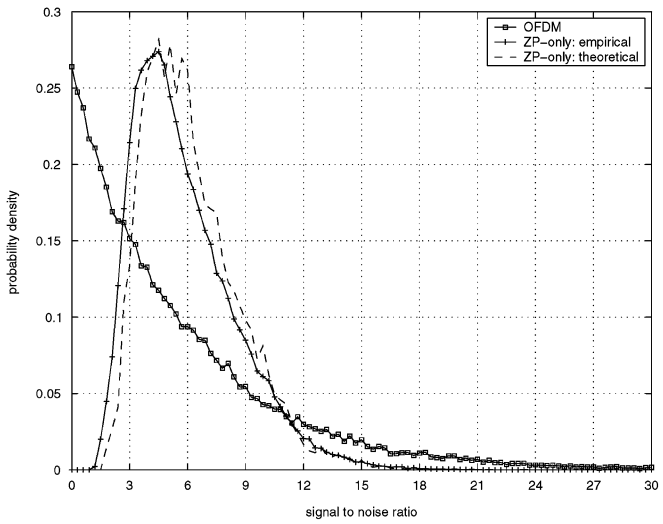

Fig. 9. PDF of the parallel channels' SNR.

coping with the additive noise. To further illuminate this point, we depict in Fig. 9 the pdf of the SNR at the parallel OFDM subchannels [cf. (3)], and the block MMSE-DFE output of ZP-only [cf. (28)] for 1000 randomly generated Model A channels at a fixed $E_b/N_0 = 10$ dB. We also depict in the same figure the empirical SNR obtained by actually measuring the SNR at the subchannels of the block MMSE-DFE[2].

We can see that in ZP-only, the SNR is more concentrated around its mean value, while in OFDM, it has both large density around zero as well as a heavy tail. In other words, the subchannels in ZP-only with block MMSE-DFE behave more like AWGN channels when compared with the OFDM ones. Both systems have an average subchannel SNR of slightly less than $10 - 10\log_{10}(3/4) = 8.75$ dB for code rate $3/4$. The loss in SNR is due to the channel dispersion and the suboptimality of MMSE-DFE (as compared with ML) for ZP-only, and due to the CP insertion in OFDM. Also, the theoretical variance of MMSE-DFE error estimates given by $\mathbf{R}_{\mathrm{ee,dfe}}^{\mathrm{zp}} = \mathbf{\Lambda}^{-1}$ is slightly (about 0.5 dB) optimistic, because our theoretical analysis ignored the error propagation.

The difference in the concentration of the SNR distributions reveals also the difference in diversity of the uncoded systems. For the rate-$3/4$ coded system, which behaves more like an uncoded system than a rate-$1/2$ coded system, the superiority of ZP-only over OFDM in performance is still quite large. For the rate-$1/2$ system, OFDM with error-control coding can pick up the loss incurred by uncoded OFDM, and outperforms the suboptimally decoded ZP-only. But from the distribution of the subchannels' SNR, we will expect ZP-only to approach or surpass OFDM in performance, using nearly optimum iterative and joint equalization/decoding, even when the code rate is low. Future work will include comparing a turbo-coded ZP-only system with the turbo-coded OFDM of [17].

Notice also that the results here are obtained with a wireless scenario in mind, where CSI is usually not available at the transmitter, and hence, the transmitter is not optimized for each channel realization. When CSI is available at the transmitter

[2]Actually, in the ZP-only case, the MMSE-DFE output still has some residual ISI, but we will treat it as additive noise here.

(e.g., in applications involving wired transmissions), multicarrier systems have been shown to outperform their single-carrier counterparts with linear or decision-feedback equalization [48], although the difference disappears as the SNR increases [53].

In practice, the wireless channel may be varying with time, which calls for adaptive channel equalization and decoding. Although OFDM is sensitive to CFO and time-varying effects, if the channel is varying slowly enough so that it can be tracked, while Doppler effects are negligible, then OFDM can enjoy advantages in adaptive equalization with its parallel subchannel structure, in addition to low-complexity decoding. In fact, even for single-carrier systems, CP extension, as in the CP-only system, has been proposed for low-complexity frequency-domain adaptive equalization [9].

VII. Conclusion

We have compared OFDM with single-carrier ZP block transmissions (that we called ZP-only) in terms of: 1) PAR; 2) sensitivity of BER performance and system throughput to frequency offsets; 3) uncoded system performance and complexity; and 4) coded system performance and complexity. The channel we considered was frequency selective and random, which is useful in predicting system performance when the fading propagation environment is slowly time varying. We focused on the case where the transmitter has no CSI, while the receiver has perfect channel information.

ZP-only has lower PAR, and its SNR degradation due to carrier frequency offsets is much less severe than that of OFDM. The throughput for both ZP-only and OFDM is not affected too much by small carrier-frequency offsets. The uncoded ZP-only enjoys a clear advantage over uncoded OFDM when the channel is random frequency selective, although the latter can afford lower receiver complexity. When error-control coding is accounted for in typical HIPERLAN/2 scenarios, coded ZP-only outperforms coded OFDM when the code rate is high, e.g., $3/4$, with a slightly higher complexity paid for block MMSE-DFE equalization. When the code rate is low and the code becomes stronger (i.e., with larger free distance), the non-ML decoding of coded ZP-only renders it inferior to an ML-decoded OFDM system which also has lower decoding complexity. From the distribution of the block MMSE-DFE output SNR, we expect ZP-only to become comparable to OFDM with near-optimum/iterative decoding, even when the code rate is low or the code is strong. Future interesting directions include comparison of single-carrier (ZP-only, CP-only, or serial) and multicarrier OFDM when multiple transmit and/or receive antennas are present.

Appendix

A. Proof of (12) and (13)

Let us define the sets $S := \{p\,|\,p \in \mathbb{C}, \Re\{p\} \leq A_{\max}, \Im\{p\} \leq A_{\max}\}$, and $S_r := \{p\,|\,p \in \mathbb{C}, |p| \leq r\}$. Considering $u(n) = x_u(n) + jy_u(n)$ with the distribution in (11), we have

$$\Pr(|u(n)| \leq r) = \iint_{S \cap S_r} dx_u dy_u.$$

Evaluating this integral in the three cases $r \leq A_{\max}$, $A_{\max} < r \leq \sqrt{2}A_{\max}$, and $r > \sqrt{2}A_{\max}$, we will obtain the result in (12). From the definition in (7), we have

$$\begin{aligned}\Pr\left(\mathrm{PAR}_i^{\mathrm{ZP}} > \gamma\right) &= \Pr\left(\|\mathbf{u}(i)\|_\infty^2 > \gamma \mathrm{E}\|\mathbf{u}(i)\|^2/P\right)\\ &= \Pr\left(\|\mathbf{u}(i)\|_\infty > \sqrt{\gamma N \bar{\sigma}_u^2/P}\right)\\ &= 1 - \prod_{k=1}^{N} \Pr\left(|[\mathbf{u}(i)]_k| \leq \sqrt{\gamma N \bar{\sigma}_u^2/P}\right)\\ &= 1 - \left[\Pr\left(|[\mathbf{u}(i)]_k| \leq \sqrt{\gamma N \bar{\sigma}_u^2/P}\right)\right]^N\end{aligned}$$

where

$$\begin{aligned}\bar{\sigma}_u^2 = \mathrm{E}[|u(n)|^2] &= \frac{1}{4A_{\max}^2} \int_{-A_{\max}}^{A_{\max}} \int_{-A_{\max}}^{A_{\max}} \left(x_u^2 + y_u^2\right)\, dx_u\, dy_u\\ &= 2A_{\max}^2/3.\end{aligned}$$

□

B. Proof of Theorem 1

We suppose ML detection with perfect CSI at the receiver and consider the PEP $\mathrm{P}(\mathbf{s} \to \mathbf{s}'\,|\,\mathbf{h}), \mathbf{s}, \mathbf{s}' \in \mathcal{A}$, that a vector $\mathbf{s}$ is transmitted but is erroneously decoded as $\mathbf{s}' \neq \mathbf{s}$. We define the set of all possible error vectors $\mathcal{A}e := \{\mathbf{e} := \mathbf{s} - \mathbf{s}'\,|\,\mathbf{s}, \mathbf{s}' \in \mathcal{A}, \mathbf{s} \neq \mathbf{s}'\}$. The PEP can be approximated using the Chernoff bound as

$$\mathrm{P}(\mathbf{s} \to \mathbf{s}'\,|\,\mathbf{h}) \leq \exp(-d^2(\mathbf{y}, \mathbf{y}')/4N_0) \tag{29}$$

where $\mathbf{y} := \mathbf{D}_H \mathbf{\Theta} \mathbf{s}, \mathbf{y}' := \mathbf{D}_H \mathbf{\Theta} \mathbf{s}'$, and $d^2(\mathbf{y}, \mathbf{y}') = \|\mathbf{y} - \mathbf{y}'\|$.

Let $r_h := \mathrm{rank}(\mathbf{R}_h)$, and the eigenvalue decomposition of $\mathbf{R}_h$ be

$$\mathbf{R}_h = [\,\mathbf{U}_1 \quad \mathbf{U}_2\,] \begin{bmatrix} \mathbf{\Sigma}_1 & \mathbf{0} \\ \mathbf{0} & \mathbf{\Sigma}_2 \end{bmatrix} \begin{bmatrix} \mathbf{U}_1^{\mathcal{H}} \\ \mathbf{U}_2^{\mathcal{H}} \end{bmatrix}$$

where $\mathbf{U}_1$ is $(L+1) \times r_h$, $\mathbf{U}_2$ is $(L+1) \times (L+1-r_h)$, $\mathbf{\Sigma}_1$ is $r_h \times r_h$ full-rank diagonal, and $\mathbf{\Sigma}_2$ is an $(L+1-r_h) \times (L+1-r_h)$ all-zero matrix. Define $\mathbf{h}_1 := \mathbf{\Sigma}_1^{-(1/2)} \mathbf{U}_1^{\mathcal{H}} \mathbf{h}$, whose Gaussian entries are i.i.d. because $\mathbf{R}_{h_1} = \mathbf{\Sigma}_1^{-(1/2)} \mathbf{U}_1^{\mathcal{H}} \mathbf{R}_h \mathbf{U}_1 \mathbf{\Sigma}_1^{-(1/2)} = \mathbf{I}_{r_h}$. It can be readily checked that, almost surely, $\mathbf{h} = \mathbf{U}_1 \mathbf{\Sigma}_1^{(1/2)} \mathbf{h}_1$.

Define now the $N \times (L+1)$ matrix $\mathbf{V}$ with $[\mathbf{V}]_{n,l} = \exp(-j2\pi nl/N)$, and use it to perform the N-point Fourier transform $\mathbf{Vh}$ of $\mathbf{h}$. Note that $\mathbf{D}_H := \mathrm{diag}(\mathbf{Vh})$. Using the definitions $\mathbf{e} := \mathbf{s} - \mathbf{s}' \in \mathcal{A}e$, $\mathbf{u}_e := \mathbf{\Theta e}$, and $\mathbf{D}_e := \mathrm{diag}(\mathbf{u}_e)$, we can write $\mathbf{y} - \mathbf{y}' = \mathbf{D}_H \mathbf{u}_e = \mathrm{diag}(\mathbf{Vh}) \mathbf{u}_e$. Furthermore, we can express the Euclidean distance $d^2(\mathbf{y}, \mathbf{y}') = \|\mathbf{D}_H \mathbf{u}_e\|^2 = \|\mathbf{D}_e \mathbf{Vh}\|^2$ as[3] $d^2(\mathbf{y}, \mathbf{y}') = \mathbf{h}_1^{\mathcal{H}} \mathbf{\Sigma}_1^{(1/2)} \mathbf{U}_1^{\mathcal{H}} \mathbf{V}^{\mathcal{H}} \mathbf{D}_e^{\mathcal{H}} \mathbf{D}_e \mathbf{V} \mathbf{U}_1 \mathbf{\Sigma}_1^{(1/2)} \mathbf{h}_1$. Defining $\mathbf{C}_e := \mathbf{V}^{\mathcal{H}} \mathbf{D}_e^{\mathcal{H}} \mathbf{D}_e \mathbf{V}$ and $\mathbf{B}_e := \mathbf{\Sigma}_1^{(1/2)} \mathbf{U}_1^{\mathcal{H}} \mathbf{C}_e \mathbf{U}_1 \mathbf{\Sigma}_1^{(1/2)}$, we have $d^2(\mathbf{y}, \mathbf{y}') = \mathbf{h}_1^{\mathcal{H}} \mathbf{B}_e \mathbf{h}_1$.

[3]For convenience, we will assume $\beta = 1$. But keep in mind that, in general, there is a power-loss factor β, except when the resulting LP-OFDM system turns out to be a ZP transmission, such as ZP-only.

Following the derivation in, e.g., [45], we can find the following upper bound on the average PEP:

$$\mathrm{P}(\mathbf{s}\to\mathbf{s}') \le \left(\frac{\mathcal{E}_{s,\mathcal{A}}}{4N_0}\right)^{-r_e}\left(\prod_{l=0}^{r_e-1}\frac{\lambda_{e,l}}{\mathcal{E}_{s,\mathcal{A}}}\right)^{-1} \tag{30}$$

where the averaging is taken over the complex Gaussian channel vector $\mathbf{h}$, r_e is the rank of $\mathbf{B}_e$, and $\lambda_{e,l}$'s are the nonzero eigenvalues of $\mathbf{B}_e$. It can be seen from (30) that for the symbol-error vector $\mathbf{e}$, r_e is the slope of the average PEP, which we denote as $G_{d,e}(\mathbf{\Theta})$, and $\prod_{l=0}^{r_e-1}(\lambda_{e,l}/\mathcal{E}_{s,\mathcal{A}}))^{1/r_e}$ gives the coding advantage, which we denote as $G_{c,e}(\mathbf{\Theta})$. Since both $G_{d,e}(\mathbf{\Theta})$ and $G_{d,c}(\mathbf{\Theta})$ depend on the choice of $\mathbf{e}$, we define the diversity and coding gains for LP block transmission systems with $\mathbf{\Theta}$, respectively, as

$$G_d(\mathbf{\Theta}) := \min_{\mathbf{e}\neq\mathbf{0}} G_{d,e}(\mathbf{\Theta}) = \min_{\mathbf{e}\neq\mathbf{0}} \mathrm{rank}(\mathbf{B}_e) \tag{31}$$

$$G_c(\mathbf{\Theta}) := \min_{\mathbf{e}\neq\mathbf{0}} G_{c,e}(\mathbf{\Theta}). \tag{32}$$

Since $\mathbf{B}_e$ is $r_h\times r_h$, its rank is, at most, r_h. It follows that the maximum diversity order is r_h, the rank of $\mathbf{R}_h$. Now we show that ZP-only can achieve the maximum diversity.

For ZP-only, $\mathbf{\Theta}$ is formed by the first K columns of an $N\times N$ FFT matrix $\mathbf{F}$; hence, $\mathbf{\Theta e}$ is the N-point FFT of $\mathbf{e}$. Using the convolution property of Fourier transforms in matrix form, we can write $\mathbf{D}_e\mathbf{V}$ as $\mathbf{FE}$, where $\mathbf{E}$ is a Toeplitz convolution matrix with first column $[\mathbf{e}^T\mathbf{0}_{1\times L}]^T$ and first row $\left[[\mathbf{e}]_1\mathbf{0}_{1,L+1}\right]$, which implements the linear convolution of a length-$(L+1)$ vector $\mathbf{h}$ with $\mathbf{e}$; thus, $\mathbf{C}_e = \mathbf{E}^{\mathcal{H}}\mathbf{F}^{\mathcal{H}}\mathbf{F}\mathbf{E} = \mathbf{E}^{\mathcal{H}}\mathbf{E}$. Since all of $\mathbf{F},\mathbf{E},\mathbf{U}_1$, and $\mathbf{\Sigma}_1^{(1/2)}$ have full column rank, it can be seen that for a length-r_h vector $\mathbf{x}$, $\mathbf{FEU}_1\mathbf{\Sigma}_1^{(1/2)}\mathbf{x} = \mathbf{0}_{N,1}$ implies that $\mathbf{x} = \mathbf{0}_{r_h,1}$; that is, $\mathbf{FEU}_1\mathbf{\Sigma}_1^{(1/2)}$ has full column rank r_h. The Gram matrix $\mathbf{B}_e$ of $\mathbf{FEU}_1\mathbf{\Sigma}_1^{(1/2)}$, therefore also has rank r_h, which implies that ZP-only can achieve maximum diversity order.

Now, we continue to establish the claim on ZP-only's maximum coding gain. When the maximum diversity order r_h is achieved, the coding gain becomes

$$\begin{aligned} G_c(\mathbf{\Theta}) &= \min_{\mathbf{e}\neq\mathbf{0}}[\det(\mathbf{B}_e)]^{\frac{1}{r_h}}/\mathcal{E}_{s,\mathcal{A}} \\ &= \min_{\mathbf{e}\neq\mathbf{0}}\left[\det(\mathbf{\Sigma}_1)\det\left(\mathbf{U}_1^{\mathcal{H}}\mathbf{C}_e\mathbf{U}_1\right)\right]^{1/r_h}/\mathcal{E}_{s,\mathcal{A}}. \end{aligned} \tag{33}$$

To maximize the coding gain, we should maximize $\det(\mathbf{U}_1^{\mathcal{H}}\mathbf{C}_e\mathbf{U}_1)$. This is, in general, difficult when $\mathbf{U}_1$ is not square, that is, when $\mathbf{R}_h$ is rank deficient. However, when $\mathbf{R}_h$ has full rank, i.e., $r_h = L+1, \mathbf{U}_1$ is a unitary matrix, $\det(\mathbf{U}_1^{\mathcal{H}}\mathbf{C}_e\mathbf{U}_1) = \det(\mathbf{C}_e)$, and $\det(\mathbf{\Sigma}_1) = \det(\mathbf{R}_h)$.

By the definition of $\mathbf{C}_e$, it can be verified that it is a Toeplitz matrix whose diagonal entries are all equal to $\mathrm{tr}(\mathbf{D}_e^{\mathcal{H}}\mathbf{D}_e) = \|\mathbf{\Theta e}\|^2$. Using the Hadamard inequality, we obtain that $\det(\mathbf{C}_e) \le \|\mathbf{\Theta e}\|^{2(L+1)}$. Letting $\boldsymbol{\theta}_k$ denote the kth column of $\mathbf{\Theta}$, we have $\|\boldsymbol{\theta}_k\| \le 1$, for some $k\in[0,K-1]$, since $\mathrm{tr}(\mathbf{\Theta}^{\mathcal{H}}\mathbf{\Theta}) = K$. Now consider the single-error events $\mathbf{e}_k = [\mathbf{0}_{k-1,1}d_{\min,\mathcal{A}}\mathbf{0}_{K-k,1}]^T, k\in[0,K-1]$, each of which has only one nonzero element at the kth position, which is $d_{\min,\mathcal{A}}$. We have $\min_{\mathbf{e}\neq\mathbf{0}}\det(\mathbf{C}_e) \le \min_k\|\mathbf{\Theta e}_k\|^{2(L+1)} = \min_k\|d_{\min,\mathcal{A}}\boldsymbol{\theta}_k\|^{2(L+1)} \le d_{\min,\mathcal{A}}^{2(L+1)}$. Therefore, the coding gain $G_c(\mathbf{\Theta})$ is upper bounded by [cf. (33)]

$$\left[\det(\mathbf{\Sigma}_1)d_{\min,\mathcal{A}}^{2(L+1)}\right]^{\frac{1}{L+1}}\Big/\mathcal{E}_{s,\mathcal{A}} = [\det(\mathbf{R}_h)]^{\frac{1}{L+1}}d_{\min,\mathcal{A}}^2\Big/\mathcal{E}_{s,\mathcal{A}}.$$

To show that ZP-only achieves this upper bound of the coding gain, we need $\det(\mathbf{C}_e) = \det(\mathbf{E}^{\mathcal{H}}\mathbf{E}) \ge d_{\min,\mathcal{A}}^{2(L+1)}$ for any error event $\mathbf{e}$. We decompose $\mathbf{E}$ as $[\mathbf{E}_1^T\mathbf{E}_2^T]^T$, where $\mathbf{E}_1$ has a few leading zero rows followed by an $(L+1)\times(L+1)$ lower triangular matrix whose diagonal entries are all equal to the first nonzero symbol, say e_j, in the error event $\mathbf{e}$. Then $\det(\mathbf{C}_e)$ becomes $\det(\mathbf{E}_1^{\mathcal{H}}\mathbf{E}_1 + \mathbf{E}_2^{\mathcal{H}}\mathbf{E}_2)$. Matrix $\mathbf{E}_1$ is nonsingular because all its diagonal entries are nonzero. Hence, $\mathbf{E}_1^{\mathcal{H}}\mathbf{E}_1$ is positive definite, while $\mathbf{E}_2^{\mathcal{H}}\mathbf{E}_2$ is, in general, positive semidefinite. Therefore, $\mathbf{E}_1^{\mathcal{H}}\mathbf{E}_1$ and $\mathbf{E}_2^{\mathcal{H}}\mathbf{E}_2$ can be simultaneously diagonalized by a matrix $\mathbf{T}$ as (see, e.g., [20])

$$\begin{aligned} \mathbf{T}^{\mathcal{H}}\mathbf{E}_1^{\mathcal{H}}\mathbf{E}_1\mathbf{T} &= \mathbf{I}_K \\ \mathbf{T}^{\mathcal{H}}\mathbf{E}_2^{\mathcal{H}}\mathbf{E}_2\mathbf{T} &= \mathrm{diag}(\lambda_0,\ldots,\lambda_{K-1}) \end{aligned}$$

where λ_k's are the nonnegative generalized eigenvalues satisfying $\mathbf{E}_2^{\mathcal{H}}\mathbf{E}_2\mathbf{t}_k = \lambda_k\mathbf{E}_1^{\mathcal{H}}\mathbf{E}_1\mathbf{t}_k, \mathbf{t}_k \neq \mathbf{0}$. Thus, $\det[\mathbf{T}^{\mathcal{H}}(\mathbf{E}_1^{\mathcal{H}}\mathbf{E}_1 + \mathbf{E}_2^{\mathcal{H}}\mathbf{E}_2)\mathbf{T}] = \prod_{k=0}^{K-1}(1+\lambda_k) \ge 1 = \det(\mathbf{I}_K) = \det(\mathbf{T}^{\mathcal{H}}\mathbf{E}_1^{\mathcal{H}}\mathbf{E}_1\mathbf{T})$. Factoring the $\det(\mathbf{T}^{\mathcal{H}})$ and $\det(\mathbf{T})$ out, we obtain the desired result

$$\begin{aligned} \det(\mathbf{C}_e) &= \det\left(\mathbf{E}_1^{\mathcal{H}}\mathbf{E}_1 + \mathbf{E}_2^{\mathcal{H}}\mathbf{E}_2\right) \ge \det\left(\mathbf{E}_1^{\mathcal{H}}\mathbf{E}_1\right) \\ &= [\det(\mathbf{E}_1)]^2 = |e_j|^{2(L+1)} \ge d_{\min,\mathcal{A}}^{2(L+1)}. \end{aligned}$$

Our proof is irrespective of N and K, as long as $N > L$ (otherwise, $\mathbf{B}_e$ will lose rank). In other words, the maximum diversity order and coding gain are both achieved by ZP-only transmissions of any block size. □

ACKNOWLEDGMENT

The authors would like to thank the anonymous reviewers for their comments and suggestions, which helped improve the quality of the paper.

REFERENCES

[1] *IEEE Standard for Wireless LAN Medium Access Control (MAC) and Physical Layer (PHY) Specifications*, IEEE 802.11, Nov. 1997.

[2] N. Al-Dhahir and A. H. Sayed, "The finite-length multi-input multi-output MMSE-DFE," *IEEE Trans. Signal Processing*, vol. 48, pp. 2921–2936, Oct. 2000.

[3] V. Aue, G. P. Fettweis, and R. Valenzuela, "A comparison of the performance of linearly equalized single carrier and coded OFDM over frequency selective fading channels using the random coding technique," in *Proc. Int. Conf. Communications*, vol. 2, Atlanta, GA, 1998, pp. 753–757.

[4] A. R. S. Bahai, M. Singh, A. J. Goldsmith, and B. R. Saltzberg, "A new approach for evaluating clipping distortion in multicarrier," *IEEE J. Select. Areas Commun.*, vol. 20, pp. 1037–1046, May 2002.

[5] L. J. Cimini, Jr., "Analysis and simulation of a digital mobile channel using orthogonal frequency-division multiplexing," *IEEE Trans. Commun.*, vol. COM-33, pp. 665–675, July 1985.

[6] L. J. Cimini, Jr. and N. R. Sollenberger, "Peak-to-average power ratio reduction of an OFDM signal using partial transmit sequences," *IEEE Commun. Lett.*, vol. 4, pp. 86–88, Mar. 2000.

[7] J. Cioffi, G. Dudevoir, M. Eyuboglu, and G. D. Forney, Jr., "MMSE decision feedback equalization and coding—Parts I and II," *IEEE Trans. Commun.*, vol. 43, pp. 2582–2604, Oct. 1995.

[8] J. M. Cioffi and G. D. Forney, Jr., "Canonical packet transmission on the ISI channel with Gaussian noise," in *Proc. GLOBECOM*, vol. 2, London, U. K., 1996, pp. 1405–1410.
[9] M. V. Clark, "Adaptive frequency-domain equalization and diversity combining for broadband wireless communications," *IEEE J. Select. Areas Commun.*, vol. 16, pp. 1385–1395, Oct. 1998.
[10] T. M. Cover and J. A. Thomas, *Elements of Information Theory*. New York: Wiley, 1991.
[11] A. Czylwik, "Comparison between adaptive OFDM and single-carrier modulation with frequency-domain equalization," in *Proc. Vehicular Technology Conf.*, vol. 2, Phoenix, AZ, 1997, pp. 865–869.
[12] R. Dinis and A. Gusmao, "On the performance evaluation of OFDM transmission using clipping," in *Proc. Vehicular Tech. Conf.*, vol. 5, 1999, pp. 2923–2928.
[13] N. Dinur and D. Wulich, "Peak-to-average power ratio in amplitude-clipped high-order OFDM," in *Proc. IEEE MILCOM*, vol. 2, 1998, pp. 684–687.
[14] N. Dinur and D. Wulich, "Peak-to-average power ratio in high-order OFDM," *IEEE Trans. Commun.*, vol. 49, pp. 1063–1072, 2001.
[15] *Channel Models for HIPERLAN/2 in Different Indoor Scenarios Norme ETSI*, Eur. Telecommun. Standards Inst. (ETSI), doc. 3ERI085B, 1998.
[16] *Broadband Radio Access Networks (BRAN); HIPERLAN Type 2 Technical Specification Part 1—Physical Layer*, Eur. Telecommun. Standards Inst. (ETSI), DTS/BRAN030 003-1, 1999.
[17] B. Le Floch, M. Alard, and C. Berrou, "Coded orthogonal frequency-division multiplex," *Proc. IEEE*, vol. 83, pp. 982–996, June 1995.
[18] G. D. Forney, Jr., "Maximum-likelihood sequence estimation of digital sequences in the presence of intersymbol interference," *IEEE Trans. Inform. Theory*, vol. IT-18, pp. 363–378, May 1972.
[19] G. J. Foschini and M. J. Gans, "On limits of wireless communications in a fading environment when using multiple antennas," *Wireless Pers. Commun.*, vol. 6, pp. 311–335, Mar. 1998.
[20] N. Franklin, *Matrix Theory*. New York: Dover, 2000.
[21] M. Friese, "On the achievable information rate with peak power limited," *IEEE Trans. Inform. Theory*, vol. 46, pp. 2579–2587, July 2000.
[22] G. B. Giannakis, "Filterbanks for blind channel identification and equalization," *IEEE Signal Processing Lett.*, vol. 4, pp. 184–187, June 1997.
[23] D. L. Goeckel and G. Ananthaswamy, "A Comparison of Single-Carrier and Multicarrier Methodologies for Wireless Communications from a Coding, Modulation, and Equalization Perspective,", http://www-unix.ecs.umass.edu/~goeckel/ofdm.html.
[24] B. Hassibi, "An efficient square-root algorithm for BLAST," in *Proc. Int. Conf. ASSP*, vol. 2, 2000, pp. 737–740.
[25] B. Hassibi and H. Vikalo, "On the expected complexity of sphere decoding," in *Proc. Asilomar Conf. Signals, Systems, Computers*, vol. 2, 2001, pp. 1051–1055.
[26] G. Hill and M. Faulkner, "Comparison of low-complexity clipping algorithms for OFDM," in *Proc. 13th IEEE Int. Symp. Personal, Indoor, Mobile Radio Communications*, vol. 1, 2002, pp. 227–231.
[27] A. E. Jones, T. A. Wilkinson, and S. K. Barton, "Block coding scheme for reduction of peak-to-mean envelope power ratio of multicarrier transmission schemes," *Electron. Lett.*, vol. 30, no. 25, pp. 2098–2099, Dec. 1994.
[28] T. Kailath, "A theorem of I. Schur and its impact on modern signal processing," in *Operator Theory: Advances and Applications*, I. Gohberg, Ed. Cambridge, MA: Birkhauser, 1986, vol. 18, pp. 9–30.
[29] T. Kailath, S.-Y. Kung, and M. Morf, "Displacement ranks of matrices and linear equations," *Math. Anal. Applicat.*, vol. 68, pp. 395–407, 1979.
[30] B. S. Krongold and D. L. Jones, "A new method for PAR reduction in baseband DMT systems," in *Proc. 35th Asilomar Conf. Signals, Systems, Computers*, vol. 1, 2001, pp. 502–506.
[31] B. Muquet, Z. Wang, G. B. Giannakis, M. de Courville, and P. Duhamel, "Cyclic prefixing or zero padding for wireless multicarrier transmissions?," *IEEE Trans. Commun.*, vol. 50, pp. 2136–2148, Dec. 2002.
[32] H. Ochiai and H. Imai, "On the distribution of the peak-to-average power ratio in OFDM," *IEEE Trans. Commun.*, vol. 49, pp. 282–289, Feb. 2001.
[33] ——, "Performance analysis of deliberately clipped OFDM signals," *IEEE Trans. Commun.*, vol. 50, pp. 89–101, Jan. 2002.
[34] M. Park, H. Jun, J. Cho, N. Cho, D. Hong, and C. Kang, "PAPR reduction in OFDM transmission using Hadamard transform," in *Proc. Int. Conf. Commun.*, vol. 1, 2000, pp. 430–433.
[35] K. G. Paterson, "Generalized Reed–Muller codes and power control in OFDM modulation," *IEEE Trans. Inform. Theory*, vol. 46, pp. 104–120, Jan. 2000.
[36] T. Pollet, M. V. Bladel, and M. Moeneclaey, "BER sensitivity of OFDM systems to carrier frequency offset and Wiener phase noise," *IEEE Trans. Commun.*, pp. 191–193, Feb.-Apr. 1995.
[37] J. Proakis, *Digital Communications*, 4th ed. New York: McGraw-Hill, 2001.
[38] M. Russell and G. L. Stüber, "Interchannel interference analysis of OFDM in a mobile environment," in *Proc. Vehicular Technology Conf.*, vol. 2, Chicago, IL, 1995, pp. 820–824.
[39] H. Sari, G. Karam, and I. Jeanclaude, "Transmission techniques for digital terrestrial broadcasting," *IEEE Commun. Mag.*, pp. 100–109, Feb. 1995.
[40] A. Scaglione, G. B. Giannakis, and S. Barbarossa, "Redundant filterbank precoders and equalizers—Part I: Unification and optimal designs," *IEEE Trans. Signal Processing*, vol. 47, pp. 1988–2006, July 1999.
[41] A. Stamoulis, G. B. Giannakis, and A. Scaglione, "Block FIR decision-feedback equalizers for filterbank precoded transmissions with blind channel estimation capabilities," *IEEE Trans. Commun.*, vol. 49, pp. 69–83, Jan. 2001.
[42] I. E. Telatar, "Capacity of multiantenna Gaussian channels," *Eur. Trans. Telecommun.*, vol. 10, no. 6, pp. 585–596, Nov.–Dec. 1999.
[43] P. Van Eetvelt, G. Wade, and M. Tomlinson, "Peak-to-average power reduction for OFDM schemes by selective scrambling," *Electron. Lett.*, vol. 32, pp. 1963–1964, Oct. 1996.
[44] Z. Wang and G. B. Giannakis, "Wireless multicarrier communications: Where Fourier meets Shannon," *IEEE Signal Processing Mag.*, vol. 47, pp. 29–48, May 2000.
[45] ——, "Linearly precoded or coded OFDM against wireless channel fades?," in *Proc. Workshop Signal Processing Advances in Wireless Communications*, Taoyuan, Taiwan, R.O.C., Mar. 20–23, 2001, pp. 267–270.
[46] ——, "A simple and general approach to the average and outage performance analysis in fading," *IEEE Trans. Commun.*, vol. 51, pp. 1389–1398, Aug. 2003.
[47] Z. Wang, S. Zhou, and G. B. Giannakis, "Joint coding/precoding with low-complexity turbo decoding," *IEEE Trans. Wireless Commun.*, to be published.
[48] T. J. Willink and P. H. Wittke, "Optimization and performance evaluation of multicarrier transmission," *IEEE Trans. Inform. Theory*, vol. 43, pp. 426–440, Mar. 1997.
[49] S. G. Wilson, *Digital Modulation and Coding*. Englewood Cliffs, NJ: Prentice-Hall, 1996.
[50] P. W. Wolniansky, G. J. Foschini, G. D. Golden, and R. A. Valenzuela, "V-BLAST: An architecture for realizing very high data rates over the rich-scattering wireless channel," in *Proc. ISSSE*, Pisa, Italy, Sept. 1998, pp. 295–300.
[51] D. Wulich, N. Dinur, and A. Glinowiecki, "Level clipped high-order OFDM," *IEEE Trans. Commun.*, vol. 48, pp. 928–930, June 2000.
[52] G. Wunder and H. Boche, "Upper bounds on the statistical distribution of the crest factor in OFDM transmission," *IEEE Trans. Inform. Theory*, vol. 49, pp. 488–494, Feb. 2003.
[53] N. A. Zervos and I. Kalet, "Optimized decision-feedback equalization versus optimized orthogonal frequency-division multiplexing for high-speed data transmission over the local cable network," in *Proc. Int. Conf. Communications*, vol. 2, Boston, MA, 1989, pp. 1080–1085.

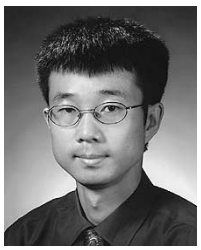

Zhengdao Wang (M'02) received the B.S. degree in electrical engineering and information science from the University of Science and Technology of China (USTC), Beijing, China, in 1996, the M.Sc. degree in electrical and computer engineering from the University of Virginia, Charlottesville, in 1999, and the Ph.D. degree in electrical and computer engineering from the University of Minnesota, Minneapolis, in 2002.

He is currently an Assistant Professor with the Department of Electrical and Computer Engineering, Iowa State University, Ames. His interests are signal processing, communications, and information theory.

Dr. Wang is the co-recipient of the 2003 IEEE Signal Processing Magazine Award.

Xiaoli Ma (M'03) received the B.S. degree in automatic control from Tsinghua University, Beijing, China, in 1998, and the M.Sc. and Ph.D. degrees in electrical engineering from the University of Virginia, Charlottesville, VA, in 1999 and the University of Minnesota, Minneapolis, MN, in 2003, respectively.

Since August 2003, she has been an Assistant Professor with the Department of Electrical and Computer Engineering, Auburn University, Auburn, AL. Her research interests include transmitter and receiver diversity techniques for wireless fading channels, communications over time- and frequency-selective channels, complex field and space–time coding, channel estimation and equalization algorithms, carrier frequency synchronization for OFDM systems, and wireless sensor networks.

Georgios B. Giannakis (S'84–M'86–SM'91–F'97) received the Diploma in electrical engineering from the National Technical University of Athens, Greece, in 1981. He received the MSc. degree in electrical engineering in 1983, M.Sc. degree in mathematics in 1986, and the Ph.D. degree in electrical engineering in 1986, from the University of Southern California (USC), Los Angeles.

After lecturing for one year at USC, he joined the University of Virginia, Charlottesville, in 1987, where he became a Professor of Electrical Engineering in 1997. Since 1999, he has been with the University of Minnesota, Minneapolis, as a Professor in the Department of Electrical and Computer Engineering, and holds an ADC Chair in Wireless Telecommunications. His general interests span the areas of communications and signal processing, estimation and detection theory, time-series analysis, and system identification, subjects on which he has published more than 180 journal papers, 340 conference papers, and two edited books. Current research focuses on transmitter and receiver diversity techniques for single- and multiuser fading communication channels, comples-field and space–time coding, multicarrier, ultra-wideband wireless communication systems, cross-layer designs, and distributed sensor networks.

Dr. Giannakis is the corecipient of five Best Paper Awards from the IEEE Signal Processing (SP) Society (1992, 1998, 2000, 2001, and 2003). He also received the Society's Technical Achievement Award in 2000. He co-organized three IEEE-SP Workshops, and guest co-edited four special issues. He has served as Editor in Chief for the IEEE SIGNAL PROCESSING L ETTERS, as Associate Editor for the IEEE TRANSACTIONS ON SIGNAL PROCESSING and the IEEE SIGNAL PROCESSING LETTERS, as secretary of the SP Conference Board, as member of the SP Publications Board, as member and vice-chair of the Statistical Signal and Array Processing Technical Committee, and as chair of the SP for Communications Technical Committee. He is a member of the Editorial Board for the PROCEEDINGS OF THE IEEE, and the steering committee of the IEEE TRANSACTIONS ON WIRELESS COMMUNICATIONS. He is a member of the IEEE Fellows Election Committee, and the IEEE-SP Society's Board of Governors.